Electronic supplementary information

A double-helical S,C-bridged tetraphenyl-*para*-phenylenediamine and its persistent radical cation

Kaho Harada,[a] Chika Hasegawa,[b] Taisuke Matsumoto,[c] Hiroki Sugishita,[a] Chitoshi Kitamura,[a] Shuhei Higashibayashi,[d] Masashi Hasegawa,[b] Shuichi Suzuki,[e] Shin-ichiro Kato*[a]

[a] *Department of Materials Science, School of Engineering, The University of Shiga Prefecture, 2500 Hassaka-cho, Hikone, Shiga 522-8533, Japan*
[b] *Department of Chemistry, School of Science, Kitasato University, 1-15-1 Kitasato, Minami-ku, Sagamihara, Kanagawa 252-0373, Japan*
[c] *Institute for Materials Chemistry and Engineering (IMCE), Kyushu University, 6-1, Kasuga-koh-en, Kasuga, Fukuoka 816-8580, Japan.*
[d] *Faculty of Pharmacy, Keio University, 1-5-30, Shibakoen, Minato-ku, Tokyo 105-8512, Japan*
[e] *Department of Chemistry, Graduate School of Engineering Science, Osaka University, 1-3 Machikaneyama-cho, Toyonaka, Osaka 560-8531, Japan*

Table of contents

1. Experimental details: synthesis of compounds

General procedures. All air-sensitive manipulations were carried out under inert nitrogen gas. An oil bath was used as the heat source. Column chromatography was carried out using SiO_2 or alumina. Thin-layer chromatography (TLC) was conducted on aluminum sheets coated with SiO_2 60 F_{254}. Melting points (M.p.) were measured with a capillary tube (Stanford Research Systems OPTiMelt MPA100). ^1H and ^{13}C NMR spectra were recorded on a spectrometer (JEOL JNM-ECS400) at 400 MHz for ^1H and 100 MHz for ^{13}C. $CDCl_3$ and *p*-xylene-d_{10} were used as a solvent, and residual solvent signal in the ^1H and ^{13}C NMR spectra was used as an internal reference. To avoid the effect of DCl_3 on the spectral broadening, Et_3N was included in $CDCl_3$. HRMS (Thermo Fisher Scientific LTQ Orbitrap XL) spectrometric analyses were conducted in a positive or negative mode. Electronic absorption (JASCO V-670 or JV-550) spectra were measured in a cuvette of 1 cm at room temperature. Cyclic voltammetry (EC Frontier ECstat-100) was performed using a cell equipped with a platinum wire working electrode, a platinum wire counter electrode, and an $Ag/AgNO_3$ reference electrode. All electrochemical measurements were performed in CH_2Cl_2 solution (ca. 0.5 mmol L^{-1}) containing 0.1 mol L^{-1} [(*n*-Bu)$_4$N][PF_6] at room temperature. All potentials are referenced to the ferrocenium/ferrocene (Fc^+/Fc) couple, which was used as a standard. EPR spectra were recorded with a JEOL JES-FE2XG spectrometer. The solutions of samples were placed in EPR tubes and degassed via the freeze–pump–thaw method, before the EPR tubes were sealed. The EPR measurements were performed using *ca.* 0.1 mmol L^{-1} solutions at room temperature. EPR spectral simulations were conducted using the Bruker program *Simfonia*. Elemental analyses were performed at A Rabbit Science Japan Co., Ltd. Quantum chemical calculations were performed by Gaussian 09 package of ab initio MO calculations.[1]

Preparation of double-helical S,C-bridged tetraphenyl-*para*-phenylenedicamine 4

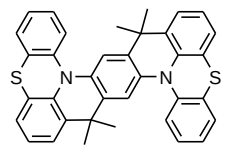

4

Diol **7** (1.54 g, 2.54 mmol) was dissolved with hot CH_2Cl_2 (200 mL). After cooling, $MeSO_3H$ (3.3 mL, 51.0 mmol, 20.0 equiv) was added to the resulting solution, and the mixture was stirred for 1 h. Aqueous NaOH was added until the solution became strongly basic. The organic phase was separated, dried over anhydrous Na_2SO_4, and evaporated under reduced pressure. The residue was dissolved with hot toluene (500 mL) and filtered through a bed of silica gel. The filtrate was evaporated under reduced pressure. The residue was successively washed with hexane (200 mL) and Et_2O (200 mL). The material collected by filtration was recrystallized from CH_2Cl_2/hexane to give *meso*-**4** (348 mg, 0.628 mmol, 24%) as a pale yellow solid. The filtrate resulting from washing with hexane and Et_2O was evaporated under reduced pressure. The residue was subjected to column chromatography (SiO_2, toluene/hexane 1:7) to give the mixture of *meso*-**4** and *rac*-**4** (193 mg, 0.349 mmol, 14%) and the pure *rac*-**4** (32.1 mg, 58.1 μmol, 2%, total yield 40%) as pale yellow solids; The ratio of *meso*-**4** to *rac*-**4** in the mixture was determined to be *ca.* 1 to 9 based on the ^1H NMR spectroscopy.

meso-**4**: M.p. 392–394 °C. ^{1}H NMR ($CDCl_3$ + Et_3N, 400 MHz) δ 7.53 (2H, s), 7.27 (2H, dd, J = 1.3 & 7.8 Hz), 7.26 (2H, dd, J = 1.6 & 7.6 Hz), 7.13 (2H, td, J = 1.4 & 7.8 Hz), 7.09 (2H, td, J = 1.6 & 7.6 Hz), 7.06 (2H, dd, J = 1.6 & 7.6 Hz), 7.06 (2H, d, J = 7.8 Hz), 7.04–7.00 (2H, m), 1.75 (6H, s), 1.13 (6H, s) ppm. ^{13}C NMR ($CDCl_3$ + Et_3N, 100 MHz) δ 143.14, 138.39, 136.35, 135.32, 135.12, 128.30, 127.52, 125.88, 124.72, 124.61, 124.08, 122.25, 118.40, 115.46, 36.69, 33.40, 22.96 ppm (17 signals out of 18 expected). UV–vis (CH_2Cl_2): λ_{max}^{abs} (ε) 360 (7800, sh), 319 (24800), 305 (20600, sh), 262 (27500) nm. HRMS (FT, positive): m/z calcd for $C_{36}H_{28}N_2S_2$ 553.1766, found 553.1770 [$(M + H)^+$].
rac-**4**: M.p. 383–384 °C. ^{1}H NMR ($CDCl_3$ + Et_3N, 400 MHz) δ 7.51 (2H, s), 7.32 (2H, dd, J = 1.1 & 8.2 Hz), 7.28 (2H, dd, J = 1.3 & 7.8 Hz), 7.23–6.97 (10H, m) 1.73 (6H, s), 1.26 (6H, s) ppm. ^{13}C NMR ($CDCl_3$ + Et_3N, 100 MHz) δ 143.36, 138.40, 136.68, 135.50, 135.33, 128.38, 127.49, 126.01, 124.68, 124.28, 123.99, 122.27, 118.24, 115.18, 36.69, 33.98, 23.16 ppm (17 signals out of 18 expected). UV–vis (CH_2Cl_2): λ_{max}^{abs} (ε) 355 (8100, sh), 322 (25100), 305 (18800, sh), 264 (27900) nm. HRMS (FT, positive): m/z calcd for $C_{36}H_{28}N_2S_2$ 553.1766, found 553.1768 [$(M + H)^+$].
Note: The UV-vis absorption spectrum of *rac*-**4** is almost consistent with that of *meso*-**4**.

Preparation of diester 6

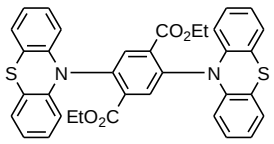

6

To the mixture of diethyl 2,5-dibromoterephthalate (**5**) (2.00 g, 5.26 mmol), CuI (803 mg, 4.21 mmol, 0.8 equiv), K_2CO_3 (2.92 g, 21.1 mmol, 4.0 equiv), and phenothiazine (2.31 g, 11.6 mmol, 2.2 equiv) was added *o*-dichlorobenzene (15 mL), which was bubbled with nitrogen for 30 min. The mixture was stirred at 180 °C for 12 h under a nitrogen atmosphere. After cooling, the resulting suspension was filtered through a bed of Celite. The filtrate was evaporated under reduced pressure. The residue was washed by Soxhlet's extractor with hexane for 12 h to give diester **6** (2.08 g, 3.37 mmol, 64%) as a deep purple solid.
M.p. 252–254 °C. ^{1}H NMR ($CDCl_3$ + Et_3N, 400 MHz) δ 8.26 (2H, s), 7.01 (4H, dd, J = 1.4 & 8.1 Hz), 6.90 (4H, td, J = 1.4 & 8.1 Hz), 6.83 (4H, td, J = 1.4 & 8.1 Hz), 6.07 (4H, dd, J = 1.4 & 8.1 Hz), 4.16 (4H, q, J = 7.6 Hz) 1.00 (6H, t, J = 7.6 Hz) ppm. ^{13}C NMR ($CDCl_3$ + Et_3N, 100 MHz) δ 164.22, 143.16, 139.98, 139.24, 138.24, 127.05, 126.87, 122.82, 119.52, 115.32, 62.37, 13.58 ppm (12 signals out of 12 expected). UV–vis (CH_2Cl_2): λ_{max}^{abs} (ε) 308 (7900), 255 (89300) nm. HRMS (FT, positive): m/z calcd for $C_{36}H_{28}N_2O_4S_2$ 616.1485, found 616.1475 [M^+].

Preparation of diol 7

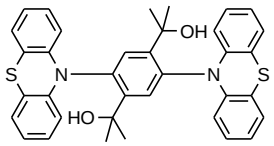

7

To a solution of diester **6** (3.04 g, 4.86 mmol) in toluene (225 mL) was added MeMgBr (3.04 mol L^{-1}, 225 mL, 58.3 mmol, 12 equiv) at room temperature under a nitrogen atmosphere. The resulting solution was stirred at 100 °C for 12 h. After the addition of ice water (200 mL), the organic phase was separated, and the aqueous phase was extracted with toluene/EtOAc (1:1, 20 mL × 16). The combined organic phase was washed with brine (25 mL × 6), dried over anhydrous Na_2SO_4, and evaporated under reduced

pressure. The residue was washed with pentane (200 mL) and collected by filtration to give diol **7** (2.24 g, 3.80 mmol, 78%) as a pale yellow solid.

M.p. 256–258 °C. ^{1}H NMR ($CDCl_3$ + Et_3N, 400 MHz) δ 7.86 (2H, s), 7.22 (4H, dd, J = 1.5 & 7.6 Hz), 7.03 (4H, td, J = 1.4 & 7.6 Hz), 6.97 (4H, td, J = 1.5 & 7.6 Hz), 6.42 (4H, dd, J = 1.4 & 7.6 Hz), 1.56 (12H, s) ppm. ^{13}C NMR ($CDCl_3$ + Et_3N, 100 MHz) δ 148.06, 145.46, 137.25, 135.38, 127.56, 127.44, 123.58, 121.60, 116.38, 72.59, 30.98 (13 signals out of 13 expected) ppm. UV–vis (CH_2Cl_2): λ_{max}^{abs} (ε) 310 (6300), 255 (78600) nm. HRMS (FT, positive): m/z calcd for $C_{36}H_{32}N_2NaO_2S_2$ 611.1797, found 611.1798 [$(M + Na)^+$].

Preparation of radical cation salt *meso*-4$^{\bullet+}$[NTf$_2$]

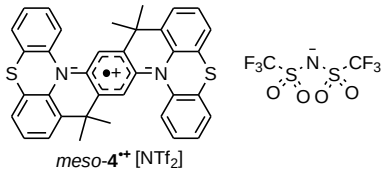
meso-**4**$^{\bullet+}$ [NTf_2]

To a solution of *meso*-**4** (30 mg, 54 μmol) in CH_2Cl_2 (40 mL) was added silver bis(trifluoromethanesulfonyl)imide (23 mg, 57 μmol, 1.05 equiv) at room temperature for a nitrogen atmosphere. After stirring for 1 h, the resulting suspension was filtered by a membrane filter. The filtrate was evaporated under reduced pressure. The residue was recrystallized from CH_2Cl_2/cyclohexane to give radical cation salt *meso*-**4**$^{\bullet+}$[NTf_2] (27 mg, 33 μmol, 60%) as dark brown crystals.

M.p. 372–374 °C. ^{1}H NMR ($CDCl_3$, 400 MHz) No peak appeared. UV–vis–NIR (CH_2Cl_2): λ_{max}^{abs} (ε) 258 (34900), 376 (6400, sh), 429 (13700), 499 (3700), 1615 (23900) nm. EPR (0.1 mM CH_2Cl_2 solution): $|a(^{14}N)|$= 0.492 mT. HRMS (ESI, positive) m/z calcd for $C_{36}H_{28}N_2S_2$ 552.1688, found 552.1690 [M^+]. HRMS (ESI, negative) m/z calcd for $C_2O_4NF_6S_2$ 279.9178, found 279.9177 [$(M–C_{36}H_{28}N_2S_2)^–$]. Anal. Calcd for $C_{38}H_{28}F_6N_3O_4S_4$: C, 54.80; H, 3.39; N 5.05. Found: C, 54.80; H, 3.49; N, 5.08.

Preparation of radical cation salt TPPD$^{\bullet+}$[NTf$_2$]

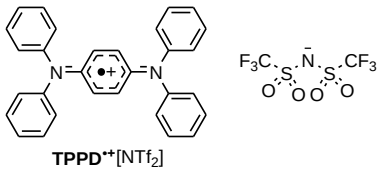
TPPD$^{\bullet+}$[NTf_2]

To a solution of *N*,*N*,*N*',*N*'-tetraphenyl-1,4-phenylenediamine (**TPPD**, 30 mg, 73 μmol) in CH_2Cl_2 (40 mL) was added silver bis(trifluoromethanesulfonyl)imide (30 mg, 76 μmol, 1.05 equiv) at room temperature for a nitrogen atmosphere. After stirring for 1 h, the resulting suspension was filtered by a membrane filter. The filtrate was evaporated under reduced pressure. The residue was recrystallized from CH_2Cl_2/cyclohexane to give radical cation salt **TPPD**$^{\bullet+}$[NTf_2] (41 mg, 60 μmol, 82%) as dark green crystals.

M.p. 168–170 °C. ^{1}H NMR ($CDCl_3$, 400 MHz) No peak appeared. UV–vis–NIR (CH_2Cl_2): λ_{max}^{abs} (ε) 257 (11500), 346 (10700), 408 (21600), 858 (18000) nm. EPR (0.1 mM CH_2Cl_2 solution): $|a(^{14}N)|$ = 0.551 mT. HRMS (ESI, positive) m/z calcd for $C_{30}H_{24}N_2$ 412.1934, found 412.1937 [M^+]. HRMS (ESI, negative) m/z calcd for $C_2O_4NF_6S_2$ 279.9178, found 279.9177 [$(M–C_{30}H_{24}N)^–$]. Anal. Calcd for $C_{32}H_{24}F_6N_3O_4S_2$: C, 55.49; H, 3.49; N 6.07. Found: C, 55.50; H, 3.58; N, 6.16.

2. X-ray crystallographic data

General procedures. Low-temperature X-ray diffraction data for *meso*-**4**, *rac*-**4**, *meso*-**4**$^{\bullet+}$**[NTf$_2$]**, and **TPPD**$^{\bullet+}$**[NTf$_2$]** were collected on a Rigaku AFC10 diffractometer coupled to a Rigaku AFC HyPix-6000 detector with Mo Kα radiation (λ = 0.71073 Å) or Cu-*K*α radiation (λ = 1.54184 Å) from an FR-E+ X-ray source. The diffraction images were processed and spaced using the CrysAlisPro software.[2] Using Olex2,[3] the structures were solved through intrinsic phasing using SHELXT[4] and refined against F^2 on all data by full-matrix least squares with SHELXL[5] following established refinement strategies. All non-hydrogen atoms were refined anisotropically. All hydrogen atoms bound to carbon were included in the model at geometrically calculated positions and refined using a riding model. The isotropic displacement parameters of all hydrogen atoms were fixed to 1.2 times the Ueq value of the atoms they are linked to (1.5 times for methyl groups).

meso-**4**: crystal data at 100 K for $C_{36}H_{28}N_2S_2$, M_r = 552.72, Orthorhombic, space group *P*na2$_1$, D_{calcd} = 1.387 g cm^{-3}, Z = 4, a = 25.8351(9) Å, b = 12.3566(5) Å, c = 8.2933(3) Å, $\alpha = \beta = \gamma = 90°$, V = 2647.50(17) Å^3; Mo-*K*α radiation, λ = 0.71073, μ = 0.232 mm^{-1}. Numbers of measured and unique reflections were 28457 [R_{int} = 0.0400, R_{sigma} = 0.0329] and 5846, respectively. Final $R(F)$ = 0.0322 for 365 parameters and 5846 reflections with $I > 2\sigma(I)$ (for all data, $R(F)$ and $wR(F^2)$ values are 0.0371 and 0.0768, respectively). CCDC-2178575.

rac-**4**: Crystal data at 100 K for $C_{36}H_{28}N_2S_2$, M_r = 552.72, Tetragonal, space group *I*-4, D_{calcd} = 1.257 g cm^{-3}, Z = 8, $a = b$ = 25.3366(5) Å, c = 9.1010(3) Å, $\alpha = \beta = \gamma = 90°$, V = 5842.3(3) Å^3; Mo-*K*α radiation, λ = 0.71073, μ = 0.210 mm^{-1}. Numbers of measured and unique reflections were 20806 [R_{int} = 0.0329, R_{sigma} = 0.0343] and 6585, respectively. Final $R(F)$ = 0.0296 for 365 parameters and 6585 reflections with $I > 2\sigma(I)$ (for all data, $R(F)$ and $wR(F^2)$ values are 0.0333 and 0.0704, respectively). CCDC-2178576.

meso-**4**$^{\bullet+}$**[NTf$_2$]**: Crystal data at 100 K for $C_{36}H_{28}N_2S_2 \cdot C_2F_6NO_4S_2 \cdot 0.5(CH_2Cl_2)$, M_r = 876.34, Monoclinic, space group *C*2/*c*, D_{calcd} = 1.564 g cm^{-3}, Z = 8, a = 31.1922(15) Å, b = 9.4751(3) Å, c = 28.2134(13) Å, $\alpha = \gamma = 90°$, β = 116.638(6)°, V = 7453.4(7) Å^3; Cu-*K*α radiation, λ = 1.54184, μ = 3.684 mm^{-1}. Numbers of measured and unique reflections were 27669 [R_{int} = 0.0793, R_{sigma} = 0.0732] and 7571, respectively. Final $R(F)$ = 0.0452 for 524 parameters and 7571 reflections with $I > 2\sigma(I)$ (for all data, $R(F)$ and $wR(F^2)$ values are 0.0730 and 0.1111, respectively). CCDC-2178577.

TPPD$^{\bullet+}$**[NTf$_2$]**: Crystal data at 100 K for $C_{32}H_{24}F_6N_3O_4S_2$, M_r = 692.66, Monoclinic, space group *C*2/*c*, D_{calcd} = 1.524 g cm^{-3}, Z = 4, a = 17.5219(3) Å, b = 7.73607(11) Å, c = 22.8391(4) Å, $\alpha = \gamma = 90°$, β = 102.7930(17)°, V = 3019.01(8) Å^3; Cu-*K*α radiation, λ = 1.54184, μ = 2.326 mm^{-1}. Numbers of measured and unique reflections were 14341 [R_{int} = 0.0336, R_{sigma} = 0.0235] and 3028, respectively.

Final $R(F)$ = 0.0413 for 272 parameters and 3028 reflections with $I > 2\sigma(I)$ (for all data, $R(F)$ and $wR(F^2)$ values are 0.0452 and 0.1167, respectively). CCDC-2178578.

3. Supporting figures, scheme, and tables

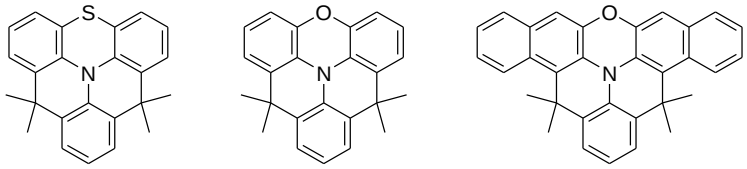

Figure S1. Chemical structures of S,C,C-bridged triphenylamine as well as O,C,C-bridged triphenylamine and dinaphtylphenylamine, which provide stable radical cations via chemical oxidation, reported by our group.[6,7]

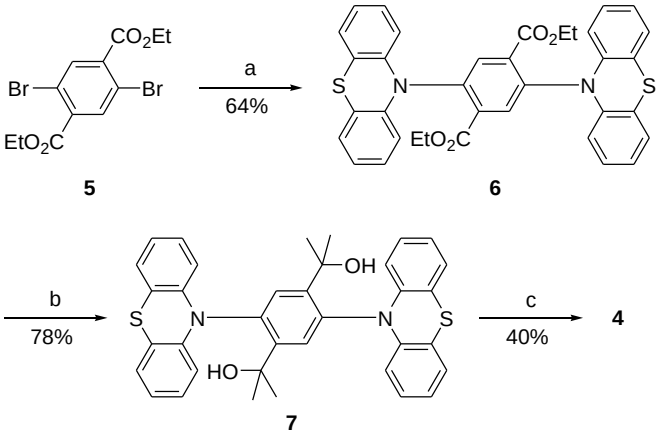

Scheme S1. Synthesis of S,C-bridged tetraphenyl-*para*-phenylenediamine **4**. *Reagents and conditions*: (a) CuI, K_2CO_3, phenothiazine, *o*-dichlorobenzene, 180 °C. (b) MeMgBr, toluene, 100 °C. (c) $MeSO_3H$, CH_2Cl_2, rt.

As shown in Scheme S1, **4** was synthesized in three steps from diethyl 2,5-dibromoterephthalate **5**. Amination of **5** with PTZ in the presence of CuI and K_2CO_3 provided diester **6** in 64% yield. The nucleophilic addition of MeMgBr to **6** followed by hydrolysis furnished diol **7** in 78% yield. Treatment of **7** with $MeSO_3H$ resulted in a two-fold Friedel–Crafts cyclization to afford **4** in 40% yield.

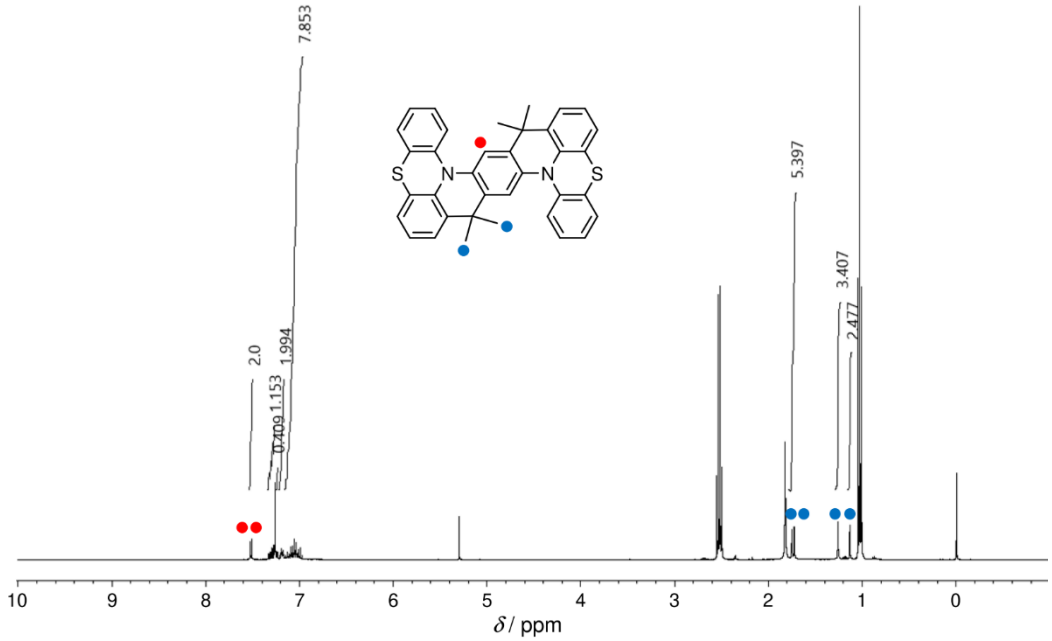

Figure S2. ^{1}H NMR spectrum of the mixture of *meso*-**4** and *racemi*-**4** in $CHCl_3/Et_3N$ solution (400 MHz).

The ratio of *meso*-**4** and *rac*-**4** in the crude product was determined to be 1.3 to 1.0 by the ^{1}H NMR spectroscopy (Figure S2).

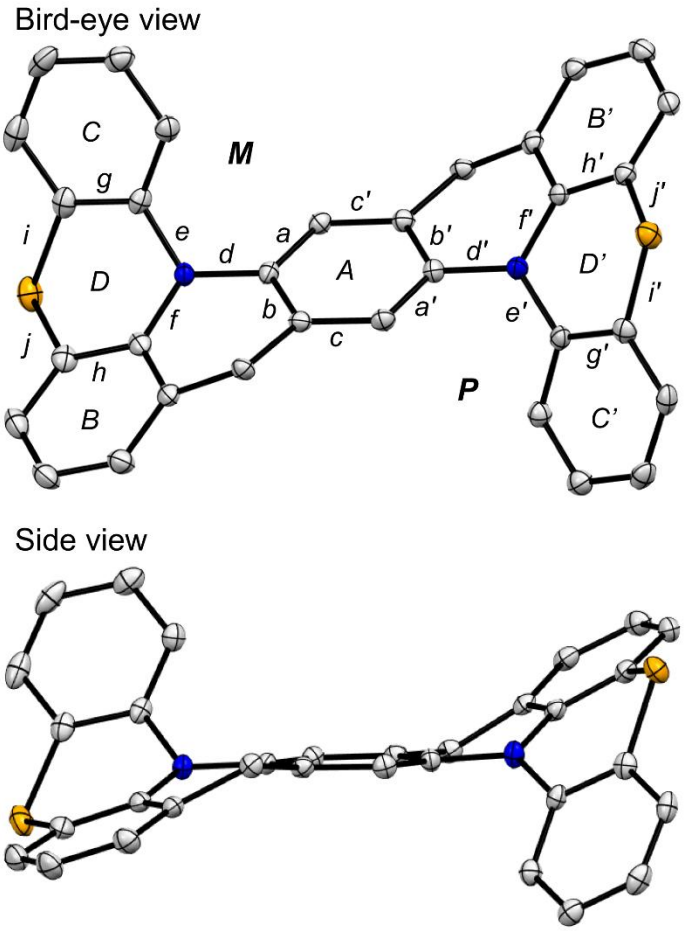

a = 1.398(3) Å
b = 1.397(3) Å
c = 1.382(3) Å
d = 1.417(3) Å
e = 1.421(3) Å
f = 1.422(3) Å
g = 1.391(3) Å
h = 1.394(3) Å
i = 1.764(3) Å
j = 1.761(3) Å

a′ = 1.387(3) Å
b′ = 1.398(3) Å
c′ = 1.391(3) Å
d′ = 1.414(3) Å
e′ = 1.410(3) Å
f′ = 1.408(3) Å
g′ = 1.393(3) Å
h′ = 1.397(3) Å
i′ = 1.759(2) Å
j′ = 1.768(2) Å

$\varphi_{A–C}$ = 63.9°
$\varphi_{A–B}$ = 20.4°
$\varphi_{B–C}$ = 49.9°
$\varphi_{A'–C'}$ = 59.2°
$\varphi_{A'–B'}$ = 31.6°
$\varphi_{B'–C'}$ = 33.2°

Figure S3. X-ray crystal structure of *meso*-**4**. Displacement ellipsoids are shown at the 50% probability level. Hydrogen atoms and Me groups are omitted for clarity.

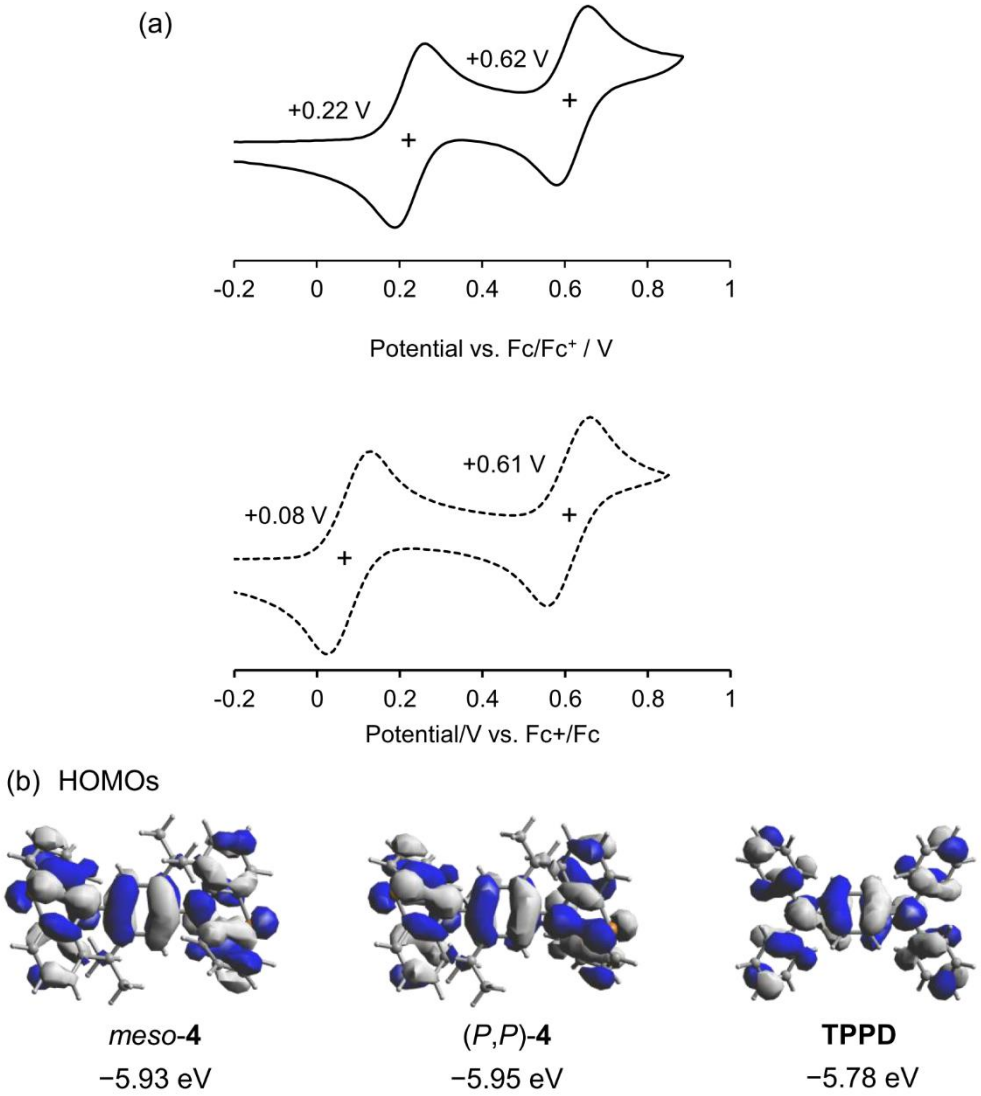

Figure S4. (a) Cyclic voltammograms of (top) *meso*-**4** and (bottom) **TPPD** at scan rate 100 mV/s in CH_2Cl_2 (0.1 mol L^{-1} [(*n*-Bu)$_4$N][PF_6]). (b) HOMOs of *meso*-**4**, (*P*,*P*)-**4**, and **TPPD** calculated at the ωB97XD/6-311+G(d,p) level of theory.

Table S1. Cyclic Voltammetry Data

Cmpd.	E_1 [V]	E_2 [V]	ΔE ($E_2 - E_1$) [V]	K_c[a]
meso-**4**	+0.22	+0.62	0.40	5.3×10^6
TPPD	+0.08	+0.61	0.53	8.0×10^8
BPB[b]	+0.28	+0.42	0.14	2.3×10^2

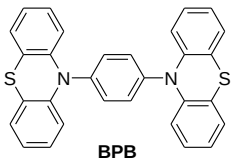

BPB

[a] Comproportionation constant of the radical cationic species.
[b] The values are taken from ref [8].

The E_1 value of *meso*-**4** is more negative than that of **BPB** (Table S1), and the ΔE of the former is larger than that of the latter. Consequently, the K_c value of *meso*-**4** is substsantially larger than that of **BPB**. These results indicate that the electronic communication between the two N atoms in *meso*-**4** is stronger than that in **BPB**, which is apparently due to the C-bridging.

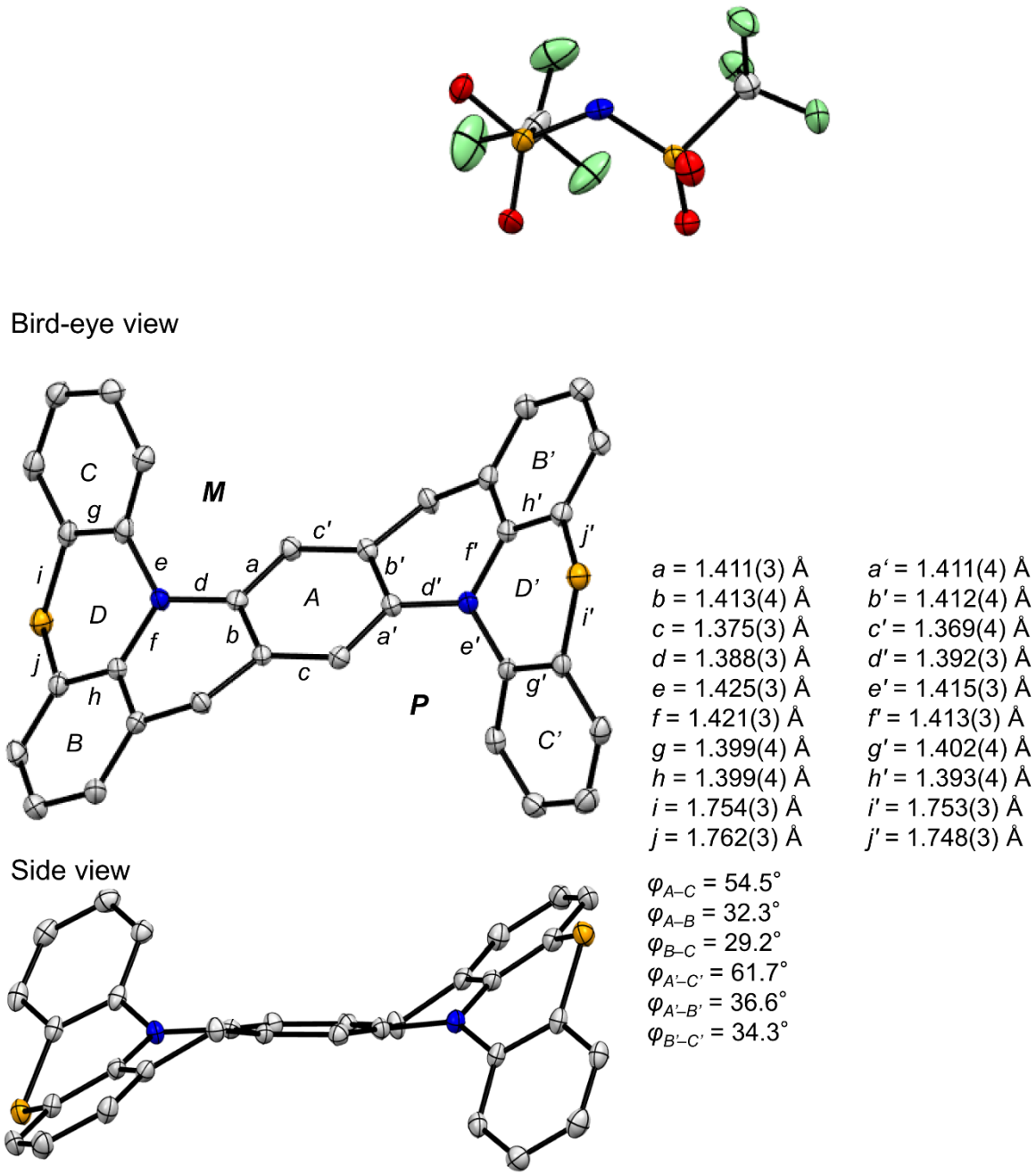

Figure S5. X-ray crystal structure of *meso*-**4**$^{\bullet+}$**[NTf$_2$]**. Displacement ellipsoids are shown at the 50% probability level. Hydrogen atoms, Me groups, and a solvent molecule are omitted for clarity.

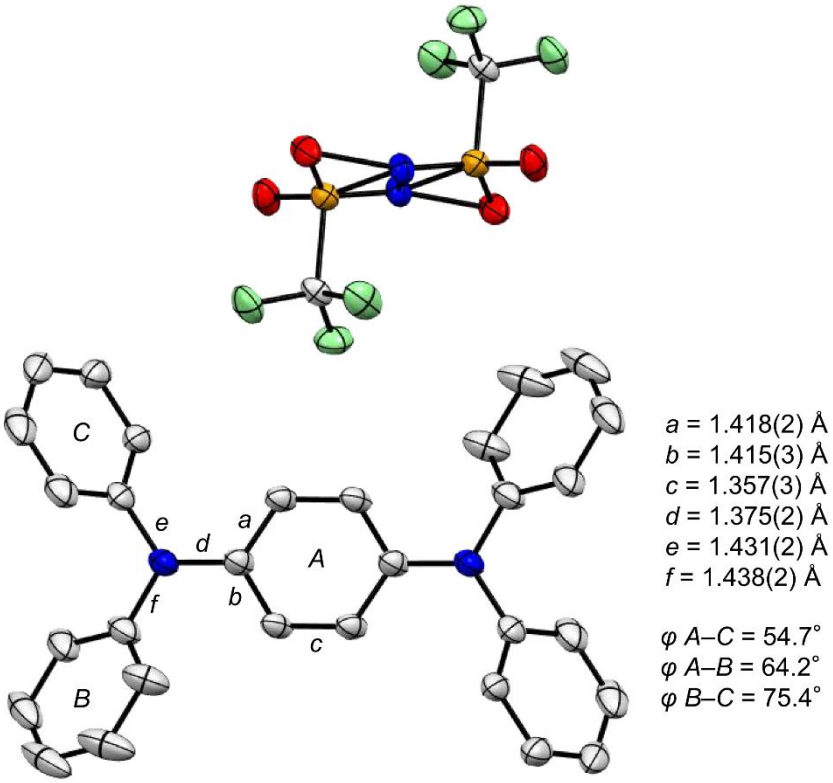

Figure S6. X-ray crystal structure of **TPPD$^{\bullet+}$[NTf$_2$]**. Displacement ellipsoids are shown at the 50% probability level. Hydrogen atoms are omitted for clarity.

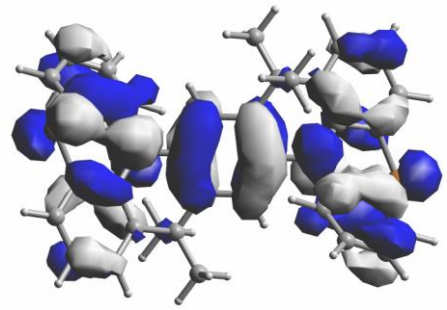

Figure S7. HOMO of *meso*-**4** calculated at the M06-2X/6-31G(d) level of theory.

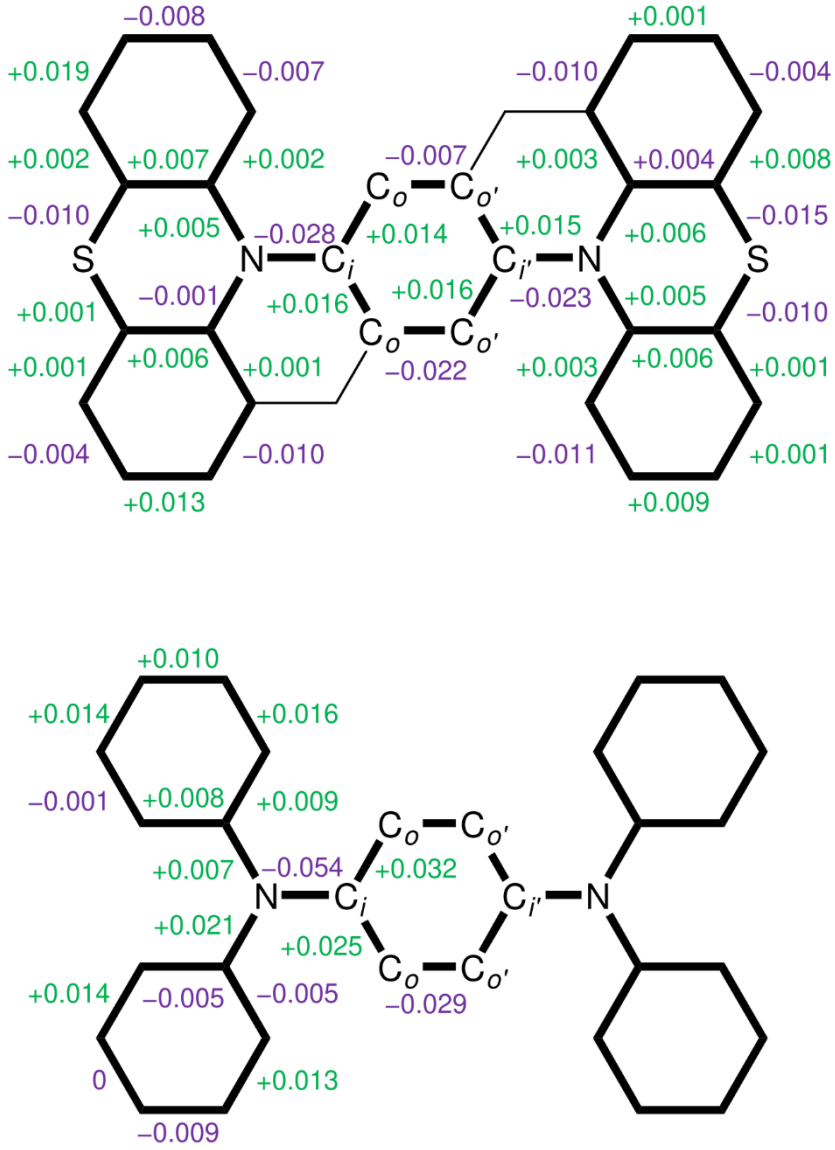

Figure S8. Averaged bond-length differences in Å for (top) *meso*-**4** and (bottom) **TPPD** upon one-electron oxidation (radical cation minus neutral). The values of bond lengths for the neutral **TPPD** are taken from ref [9].

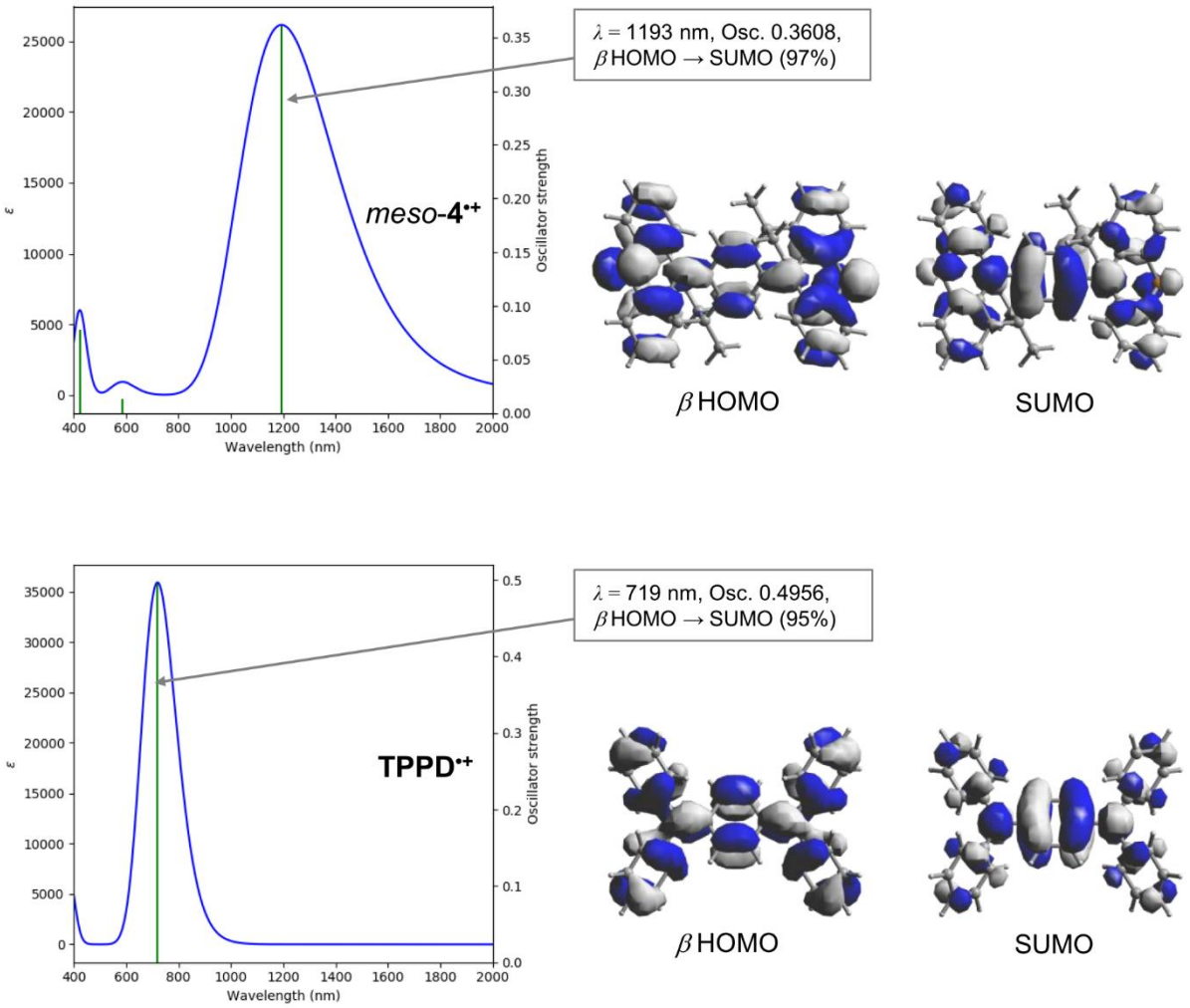

Figure S9. Results of TD-DFT calculations for *meso*-**4**$^{\bullet+}$ and **TPPD**$^{\bullet+}$ calculated at the TD-UM06-2X/6-31G(d)//UM06-2X/6-31G(d) level of theory.

Table S2. Characteristic Electron-Transfer Parameters Obtained through Mulliken–Hush Analysis of the NIR Absorption Bands [a]

Cmpd	R [Å] [b]	λ_{MH} [10^3 cm^{-1}] [c]	$\Delta\nu_{max}$ [10^3 cm^{-1}] [d]	ε [10^3 M^{-1} cm^{-1}] [e]	V_{MH} [10^3 cm^{-1}] [f]	$\Delta G^{\ddagger}$ [kcal mol^{-1}] [g]
meso-**4**$^{\bullet+}$	5.5	6.2	2.6	23.9	2.3	0.3
TPPD$^{\bullet+}$ [h]	5.6	11.3	4.3	18.0	3.5	1.2
BPB$^{\bullet+}$ [i]	5.6 [j]	10.3	3.2	0.86	0.62	5.7

[a] See ref [8]. [b] The distance between the two nitrogen atoms based on the single-crystal X-ray structures. [c] The reorganization energy that is evaluated from the IV-CT absorption band, i.e., $\lambda_{MH} = \lambda_{max}$. [d] Bandwidth at half-height. [e] Molar absorption coefficiency in the IV-CT band. [f] Electronic coupling element $V_{MH} = 0.0206 \times (\lambda_{MH} \times \Delta\nu_{max} \times \varepsilon)^{1/2} / R$. [g] Electron-transfer activation barrier = $(\lambda_{MH} - 2V_{MH})^2 / 4\lambda_{MH}$. The radical cations are hypothetically assumed to be Robin–Day class II compounds. [h] In ref [9], **TPPD**$^{\bullet+}$ is assigned to be a class III compound. [i] in ref [8], **BPB**$^{\bullet+}$ is assigned to be a class II compound. [j] In ref [8], the distance (8.6 Å) is defined as that between the centers of the two phenothiazine moieties.

We estimated the characteristic electron-transfer parameters for *meso*-**4**$^{\bullet+}$ as well as **TPPD**$^{\bullet+}$ and **BPB**$^{\bullet+}$ (Table S2). We consider that *meso*-**4**$^{\bullet+}$ is very close to the class II/III boundary, and thus the electron spin and positive charge are delocalized over almost the entire π-conjugated framework according to the following three findings.

(1) The radical cations **TPPD**$^{\bullet+}$ and **BPB**$^{\bullet+}$ are assigned to be Robin–Day class III and class II compounds, respectively, in the literature.[8,9] The V_{MH} value for *meso*-**4**$^{\bullet+}$ (2310 cm^{-1}) is slightly smaller than that for **TPPD**$^{\bullet+}$ (3450 cm^{-1}) and significantly larger than that for **BPB**$^{\bullet+}$ (620 cm^{-1}).

(2) The V_{MH} value for *meso*-**4**$^{\bullet+}$ (2310 cm^{-1}) is smaller than its $\lambda_{MH}/2$ value (3120 cm^{-1}).

(3) When both **TPPD**$^{\bullet+}$ and *meso*-**4**$^{\bullet+}$ are hypothetically assumed to be class II compounds, the $\Delta G^{\ddagger}$ value for *meso*-**4**$^{\bullet+}$ (0.3 kcal mol^{-1}) is still smaller than that for **TPPD**$^{\bullet+}$ (1.2 kcal mol^{-1}).

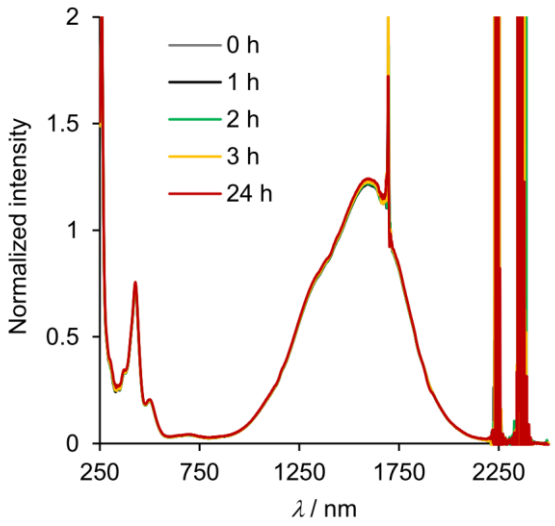

Figure S10. Time profiles of UV–vis–NIR spectra of *meso*-**4**$^{\bullet+}$**[NTf$_2$]** in CH_2Cl_2.

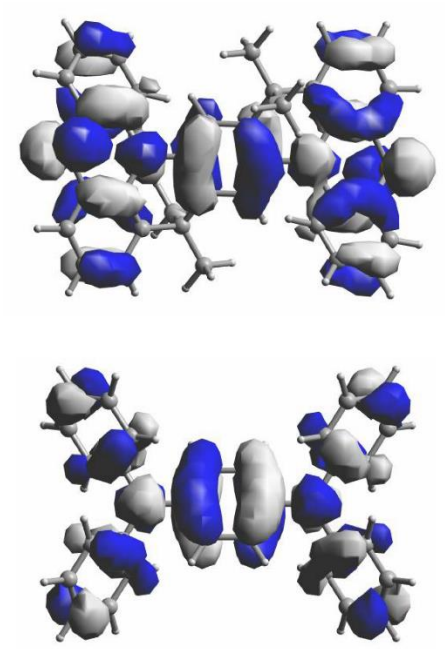

Figure S11. SOMO of (top) *meso*-**4**$^{\bullet+}$ and (bottom) **TPPD**$^{\bullet+}$ calculated at the UM06-2X/6-31G(d) level of theory.

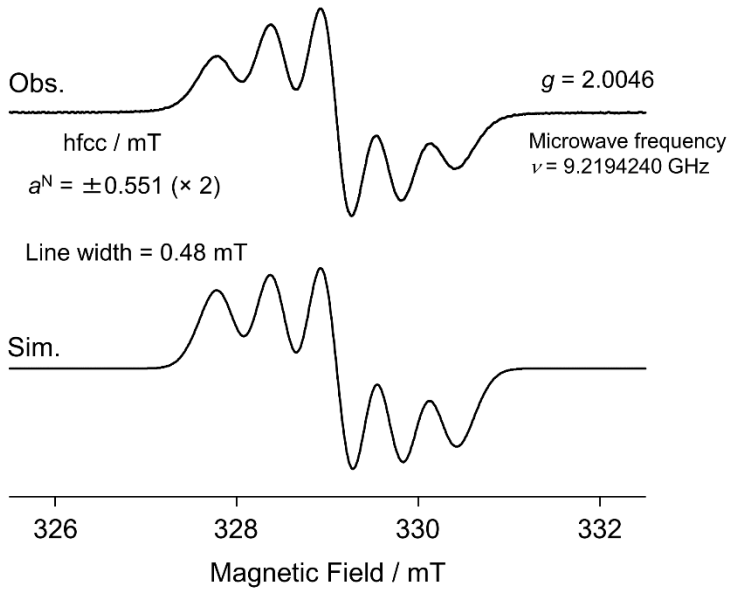

Figure S12. Experimentally observed EPR spectrum (top) of **TPPD**$^{\bullet+}$ in CH_2Cl_2 at room temperature and the simulated spectrum (bottom).

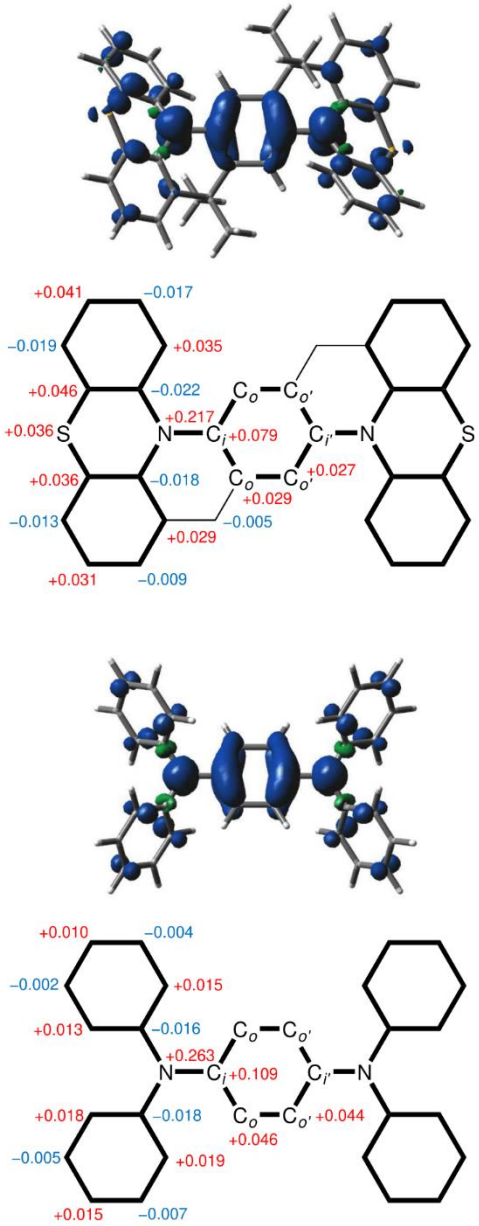

Figure S13. Spin-density map and Mulliken atomic spin density values of (top) *meso*-**4**$^{\bullet+}$ and (bottom) **TPPD**$^{\bullet+}$ calculated at the UM06-2X/6-31G(d) level of theory (isovalue: 0.005).

The Mulliken atomic spin density (MSD) value for the nitrogen atoms of *meso*-**4**$^{\bullet+}$ (+0.217) is smaller than that of the nitrogen atoms in **TPPD**$^{\bullet+}$ (+0.263) (Fig. S13). This result is consistent with the trend observed in the a_N values. The MSD values for the C_i, C_o, and $C_{o'}$ carbons of *meso*-**4**$^{\bullet+}$ are also smaller than the corresponding values found in **TPPD**$^{\bullet+}$. A subtle but distinctive MSD value is found for the sulfur atoms of *meso*-**4**$^{\bullet+}$ (+0.036). In addition, the MSD values for the carbon atoms of the *B*/*B*′–*D*/*D*′ rings in *meso*-**4**$^{\bullet+}$ (+0.029 – +0.046) are generally more positive than those observed in **TPPD**$^{\bullet+}$ (+0.010 – +0.019). This result highlights that the sulfur and carbon bridges in *meso*-**4**$^{\bullet+}$ enable the spin density to delocalize from ring *A* and the nitrogen atoms to the *B*/*B*′–*D*/*D*′ rings, namely, the PTZ moieties.

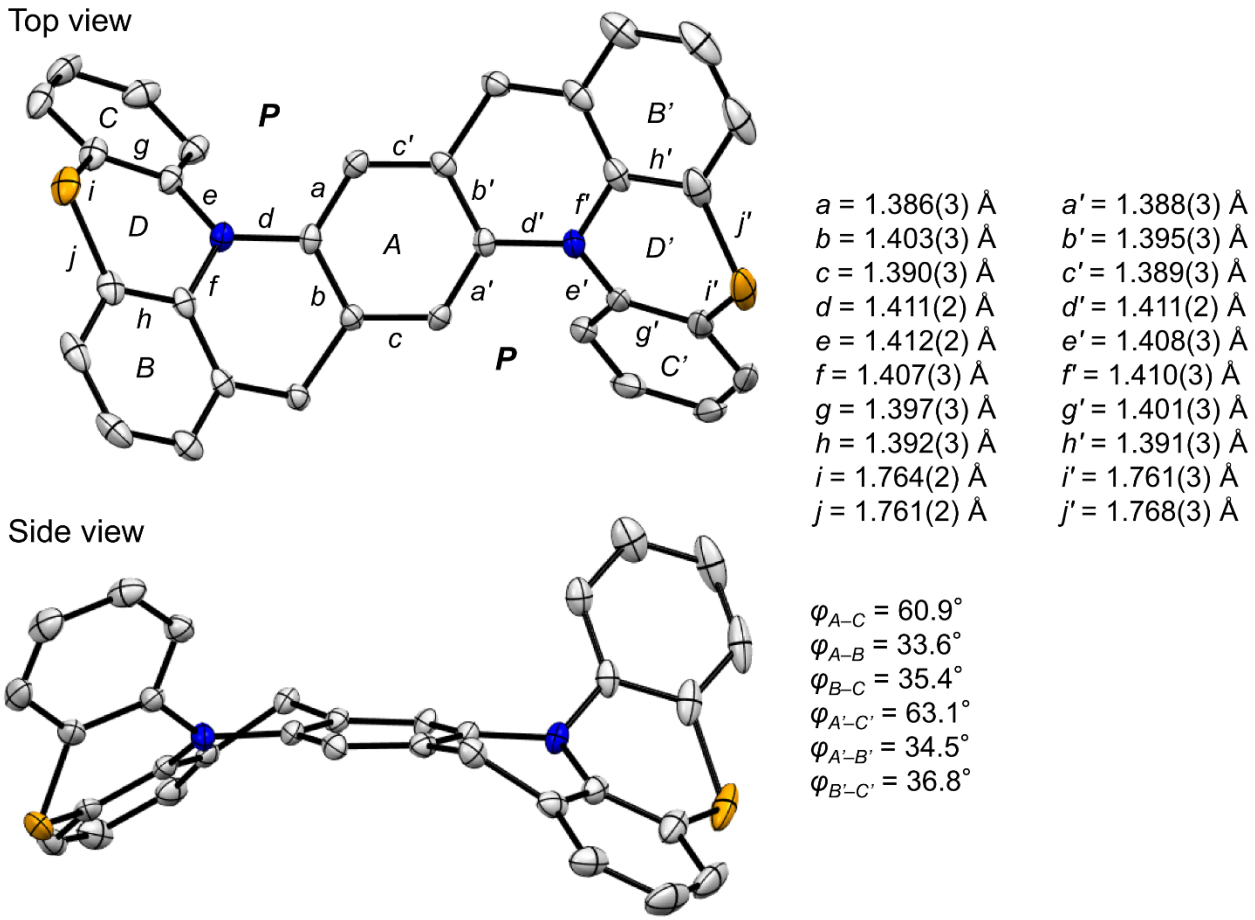

Figure S14. X-ray crystal structure of *rac*-**4**. Displacement ellipsoids are shown at the 50% probability level. Hydrogen atoms and Me groups are omitted for clarity. In the crystal of *rac*-**4**, two enantiomers, i.e., (*P*,*P*)-**4** and (*M*,*M*)-**4**, existed in the ratio of 1:1. One of the two enantiomeric molecules is shown.

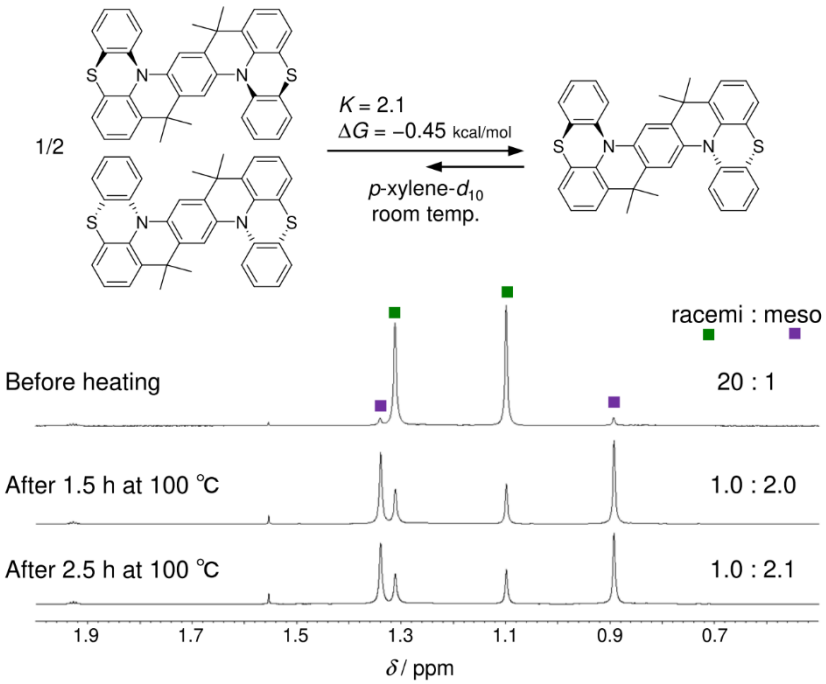

Figure S15. ^{1}H NMR spectra of **4**, which was heated at 100 °C, measured at room temperature in *p*-xylene-d_{10}.

Kinetic studies: A solution of *p*-xylene-d_{10} solution containing a large excess of *rac*-**4** was placed in a NMR tube and equilibrated at the corresponding temperature within an oil bath, and a timer was started. For each data point, the tube was taken out of the oil bath, the timer was stopped, and a ^{1}H NMR spectrum was recorded at 20 °C, after which the heating and the timer were resumed. Rate constants k at the corresponding temperature T were determined by monitoring the concentrations of disappearing *rac*-**4** and forming *meso*-**4** using ^{1}H NMR spectroscopy.

$$C_{(MMPP)} = C_{(M,M)} + C_{(P,P)}$$

$$\Longrightarrow -\frac{dC_{(MMPP)}}{dt} = (k_3 + k_4)\, C_{(MMPP)} - 2(k_1 + k_2)\, C_{(M,P)}$$

$$C_{(MM'PP')} > C_{(M,P)}$$

$$(k_3 + k_4)\, C_{(MMPP)} > 2(k_1 + k_2)\, C_{(M,P)}$$

$$\Longrightarrow -\frac{dC_{(MMPP')}}{dt} = (k_3 + k_4)\, C_{(MMPP)}$$

$C_{(MMPP'(0))}$ is the sum of the initial concentrations of $C_{(MM)}$ and $C_{(PP)}$.

$$\Longrightarrow \int_{C_{(MMPP(0))}}^{C_{(MMPP)}} -\frac{dC_{(MP)}}{(k_3 + k_4)\, C_{(MMPP)}} = \int_0^t dt$$

$$\Longrightarrow \ln\frac{C_{(MMPP'(0))}}{C_{(MMPP')}} = (k_3 + k_4)t$$

$$\Longrightarrow \ln C_{(MMPP(0))} = \ln C_{(MMPP)} - (k_3 + k_4)t$$

According to the theoretical calculations, k_3 and k_4 are regard to be nearly equal. The rate constant k for isomerization from the racemic form to the meso form can be deduced from the following equation.

$$k = \frac{k_3 + k_4}{2}$$

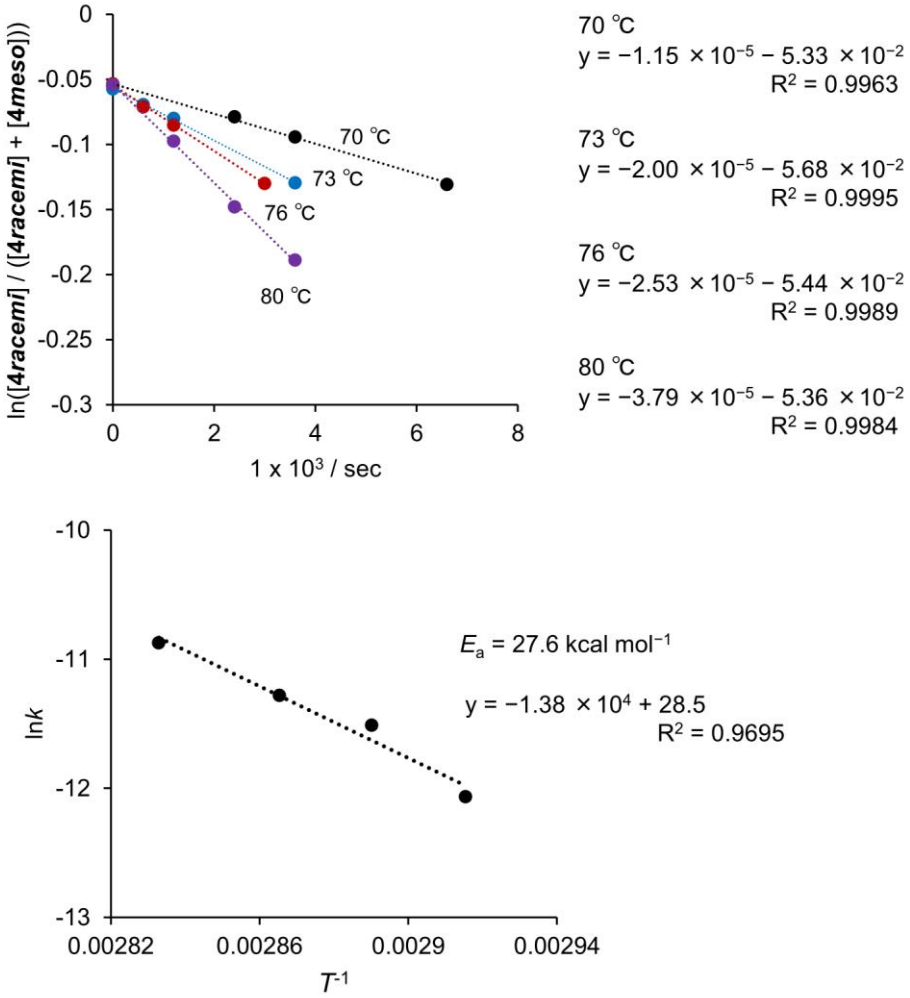

Figure S16. Isomerization kinetics from *rac*-**4** to *meso*-**4** in *p*-xylene-d_{10}. First-order plots (top) and Arrehenius plots (bottom).

Table S3. Isomerization Kinetics Data from *rac*-**4** to *meso*-**4** in *p*-xylene-d_{10}

Temp. [°C]	$k \times 10^5$ [sec^{-1}]	ln$k$
70	0.576	–17.9
73	1.00	–17.3
76	1.26	–17.1
80	1.89	–16.7

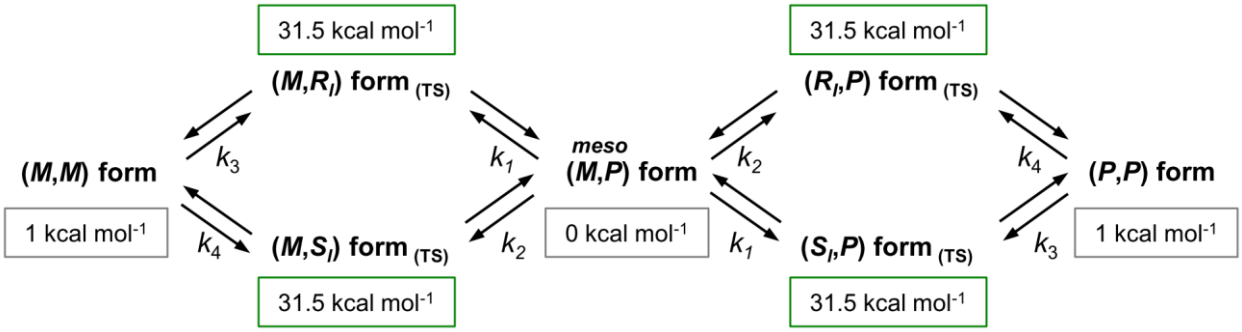

Figure S20. Potential energy diagram for the isomerization of **4** calculated at the ωB97XD/6-311+G(d,p) level of theory. The selected optimized structures are shown in Figure S21.

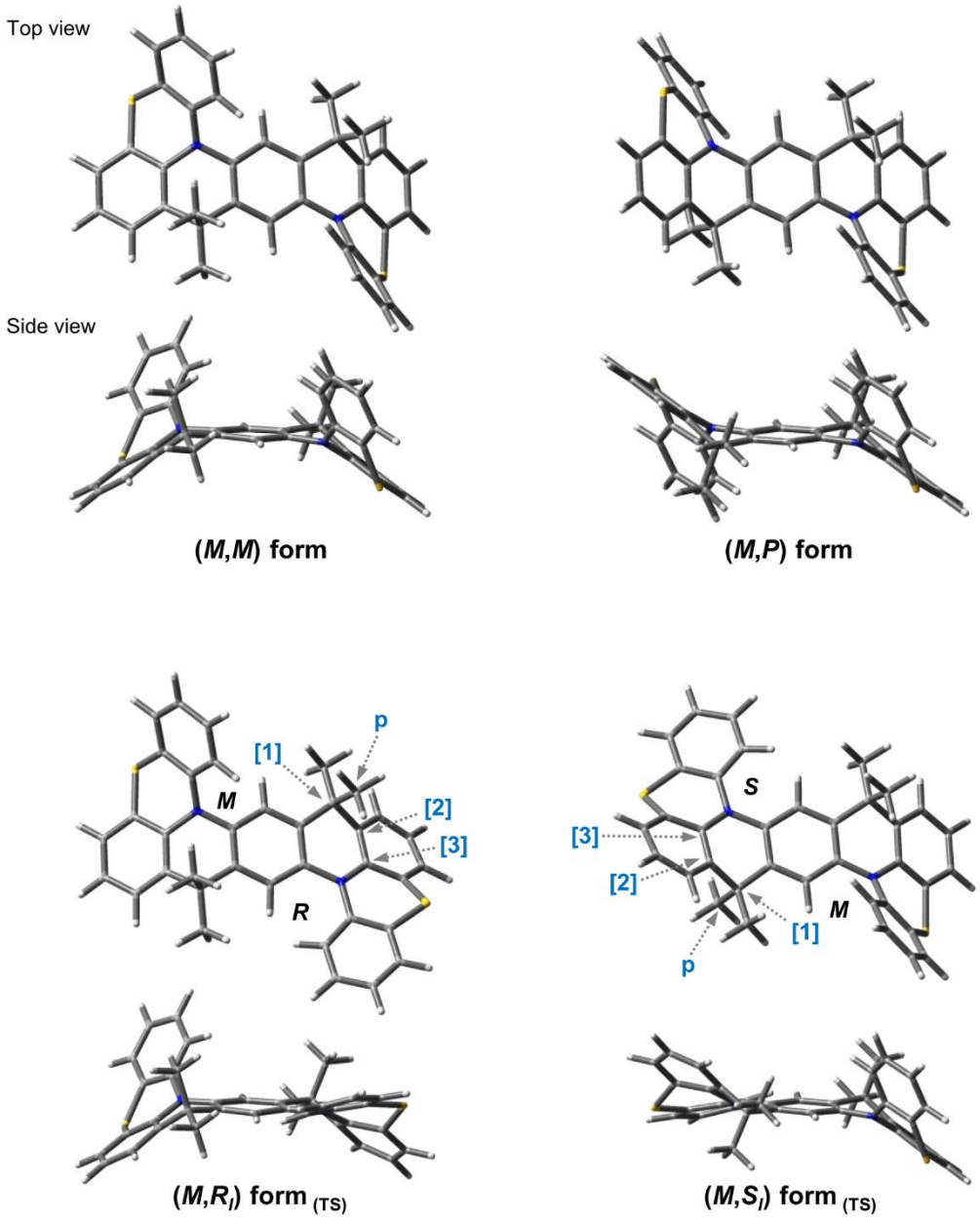

Figure S21. Optimized structures of **4** calculated at the ωB97XD/6-311+G(d,p) level of theory.

Optical resolution: The racemic mixture was separated into enantiomers by using a chiral HPLC method on a chiral stationary phase (Chiralpak IA, $\phi = 20$ mm, L = 250 mm) with the elution of CH_2Cl_2-hexane (v/v = 1:4). After three cycles, three peaks of frac.1 (black label in Figure S15), frac.2 (red label), and frac.3 (blue label) were collected. From the NMR measurements, frac.1 was determined as *meso*-**4** and frac.2 and frac.3 were enantiomers of **4**. The absolute configuration of these fractions was determined by the comparison of experimental CD spectra and simulated optical rotation obtained from TD-DFT calculations. As a result, frac. 2 (faster) and frac. 3 (slower) were determined to be (*P*,*P*)-**4** and (*M*,*M*)-**4**, respectively.

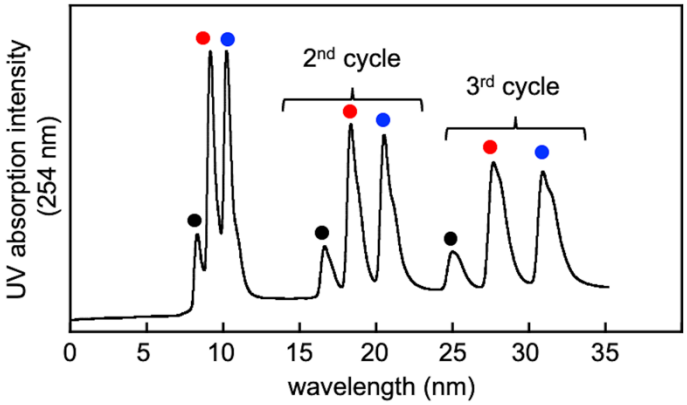

Figure S22. Chromatogram for the resolution of *rac*-**4** using UV (254 nm) detector.

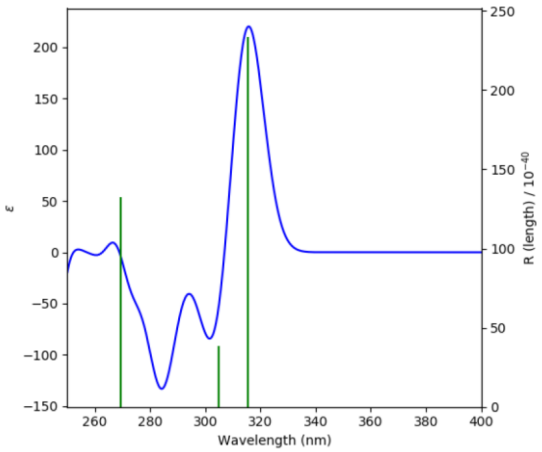

Figure S23. Results of TD-DFT calculations for (*M*,*M*)-**4** calculated at the TD-CAM-B3LYP/def2TZVP//ωB97XD/6-311+G(d,p) level of theory.

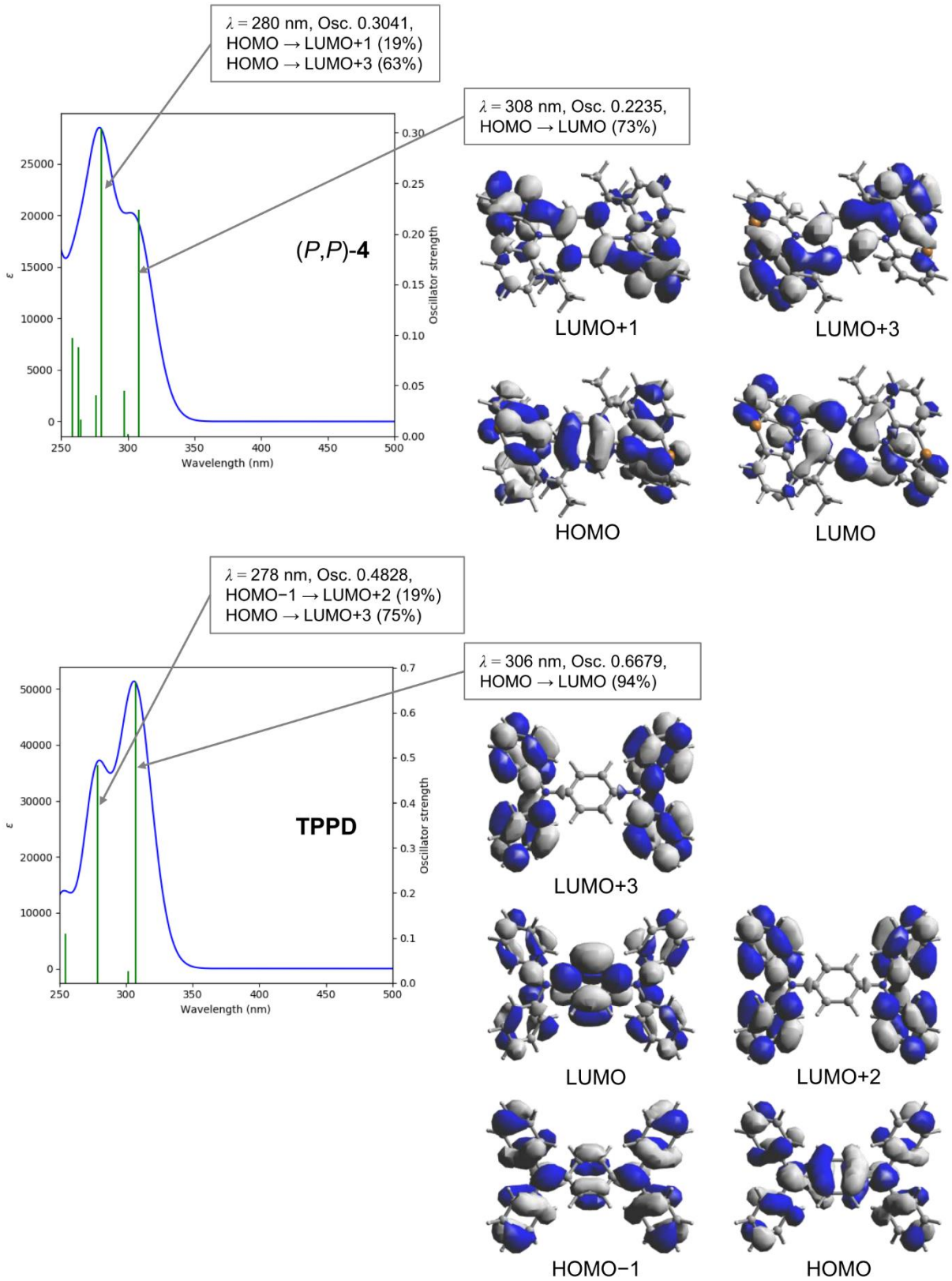

Figure S24. Results of TD-DFT calculations for (*P*,*P*)-**4** and **TPPD** calculated at the TD-M06-2X/6-31G(d)//M06-2X/6-31G(d) level of theory.

Table S4. Calculated Total Energies of Triplet and Singlet States, and the Intermolecular Exchange Interactions (J_{inter_calc}/k_B) for the Dication *meso*-$\mathbf{4}^{2+}$ [a]

Spin State	E [au]	$<S^2>$	$2J_{inter\_calc}/k_B$ [K]
HS ($S = 1$)	–2294.1210926	2.012243	–1413.1
LS ($S = 0$)	–2294.1235969	0.893026	

[a] The total energies were calculated by using density functional theory at the UB3LYP level of theory with 6-31G(d,p) basis set for C, H, N, S.[1] The total energy calculated using UHF-SCF procedure involving spin contamination due to the higher spin states. In order to estimate the exchange interaction, a compensation equation was used, $J_{inter\_calc} = ({}^{LS}E - {}^{HS}E)/(<{}^{HS}S^2> - <{}^{LS}S^2>)$.[10]

4. ^{1}H and ^{13}C NMR data

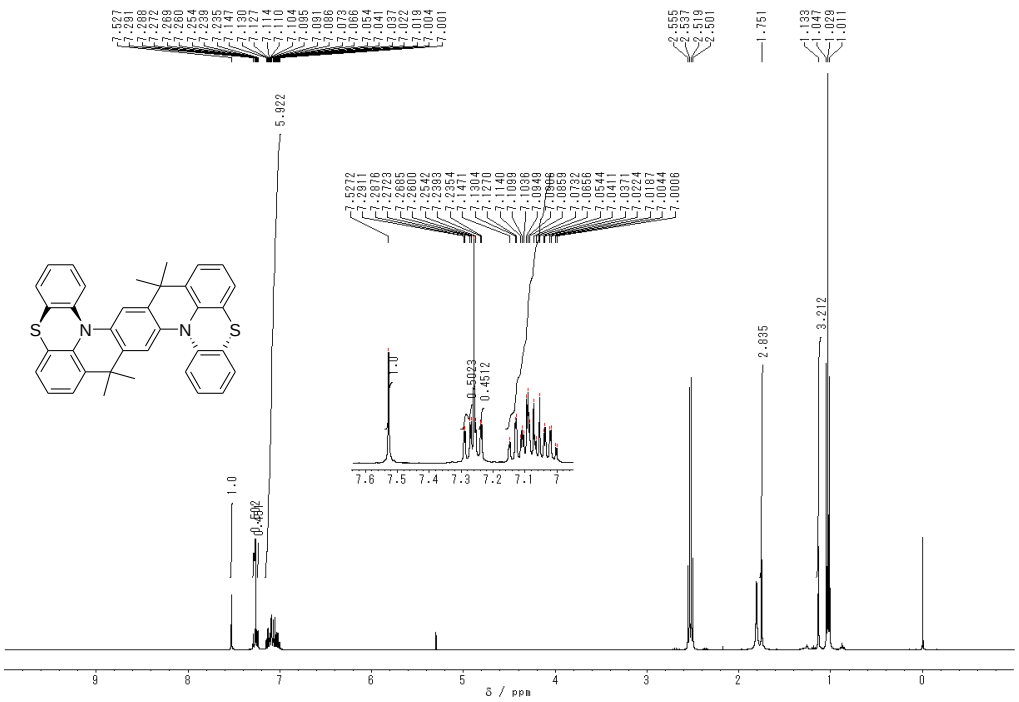

Figure S25. ^{1}H NMR spectrum of *meso*-**4** in $CDCl_3/Et_3N$ solution (400 MHz).

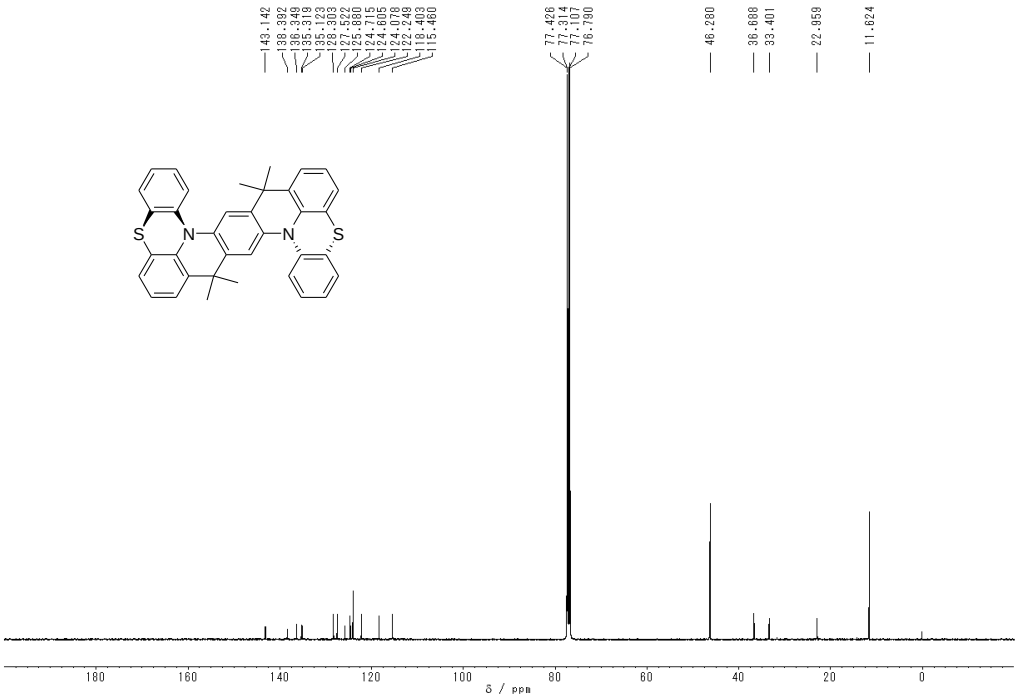

Figure S26. ^{13}C NMR spectrum of *meso*-**4** in $CDCl_3/Et_3N$ solution (100 MHz).

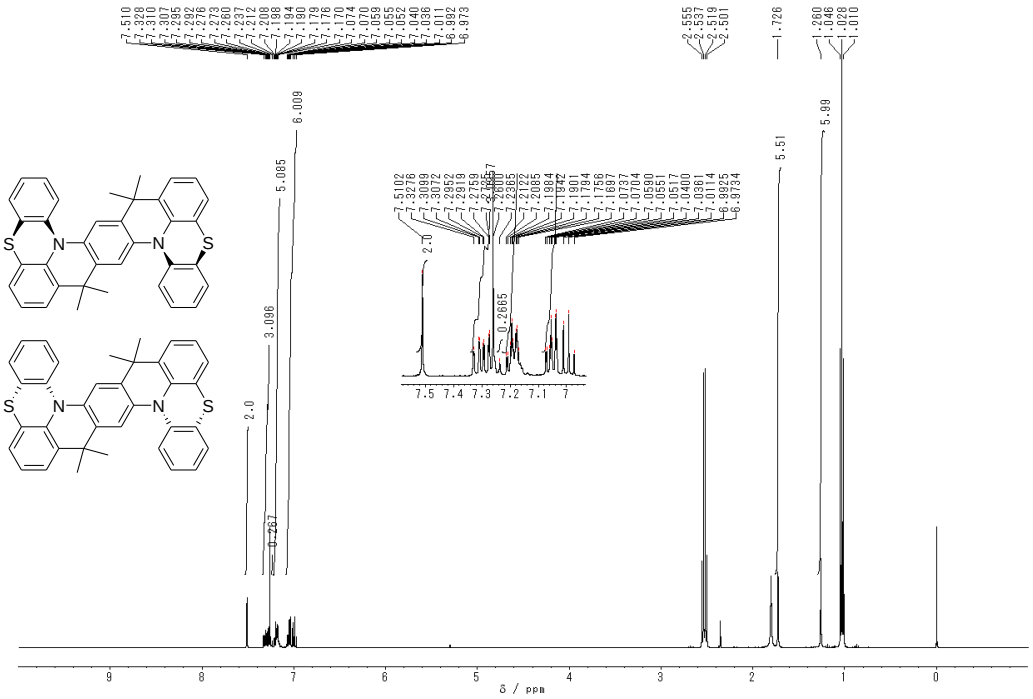

Figure S27. ^{1}H NMR spectrum of *rac*-**4** in $CDCl_3/Et_3N$ solution (400 MHz).

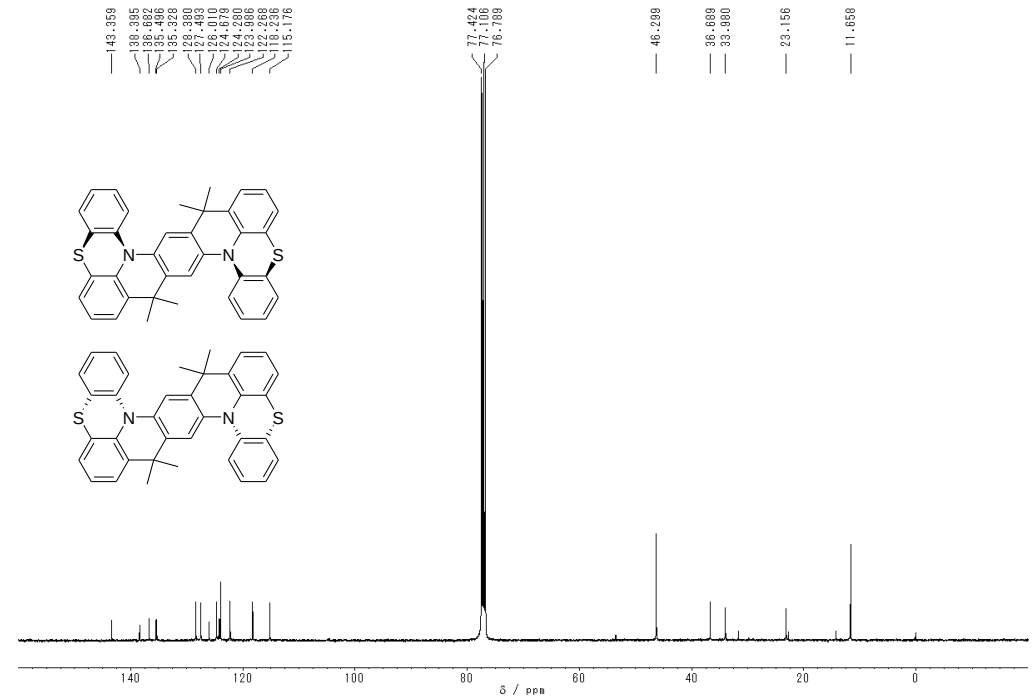

Figure S28. ^{13}C NMR spectrum of *rac*-**4** in $CDCl_3/Et_3N$ solution (100 MHz).

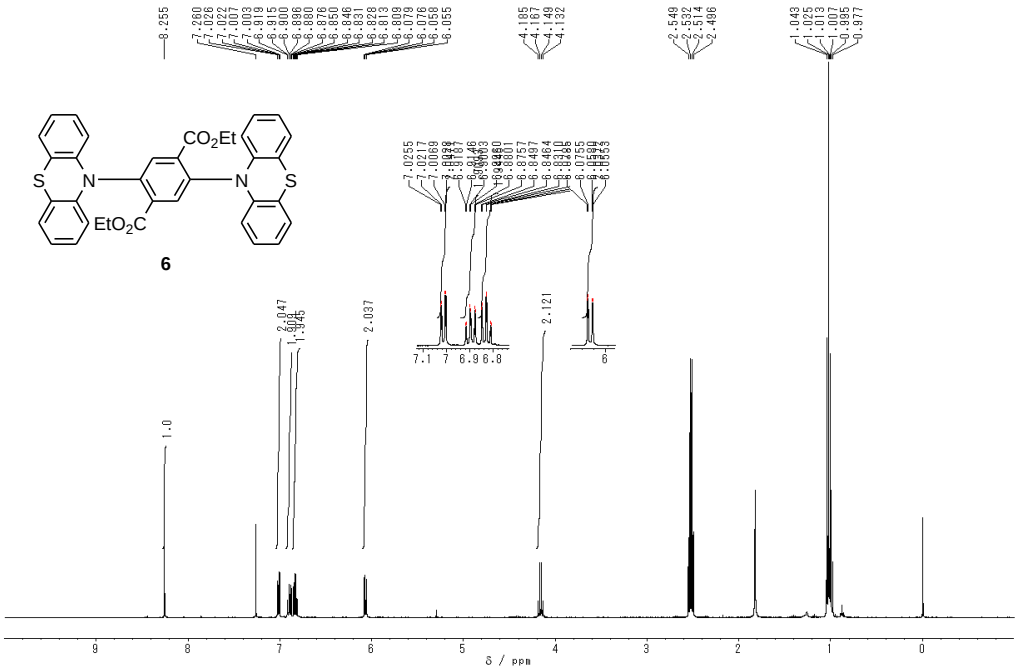

Figure S29. ^{1}H NMR spectrum of **6** in $CDCl_3/Et_3N$ solution (400 MHz).

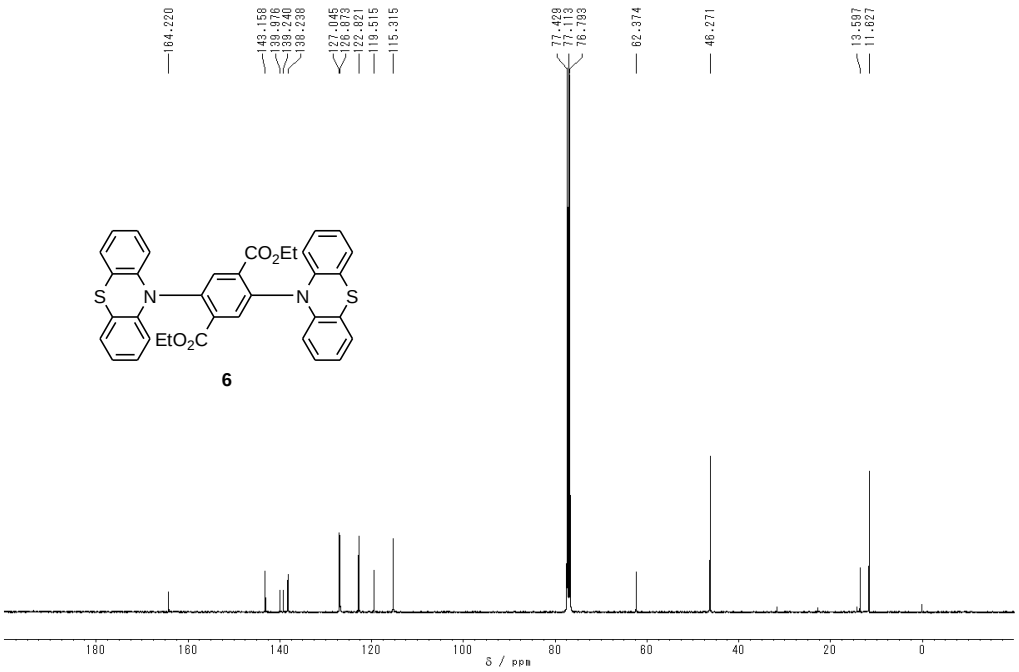

Figure S30. ^{13}C NMR spectrum of **6** in $CDCl_3/Et_3N$ solution (100 MHz).

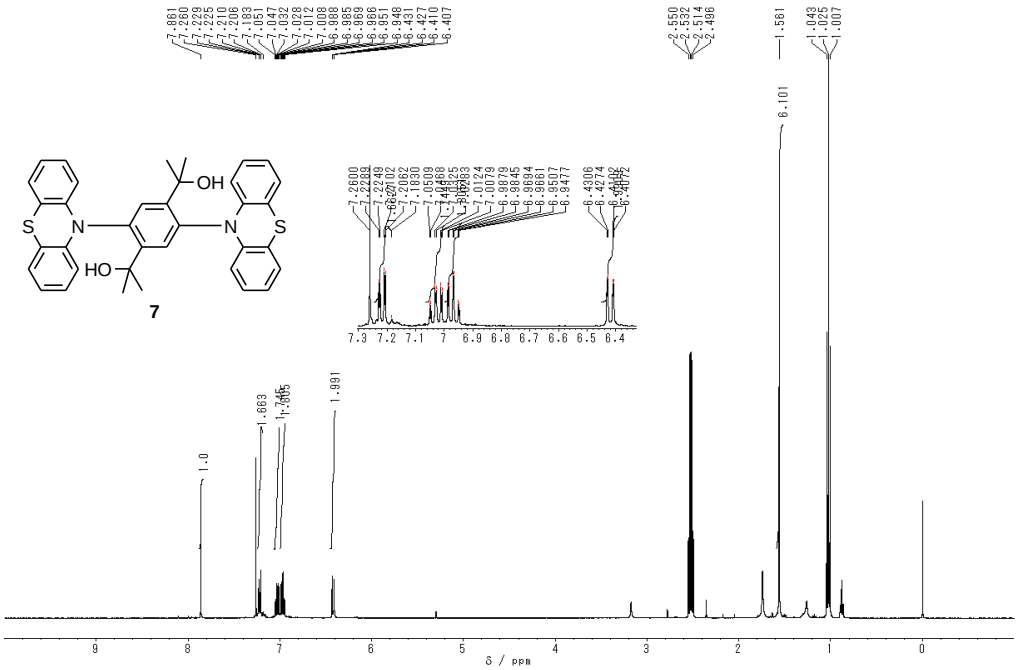

Figure S31. ^{1}H NMR spectrum of **7** in $CDCl_3/Et_3N$ solution (400 MHz).

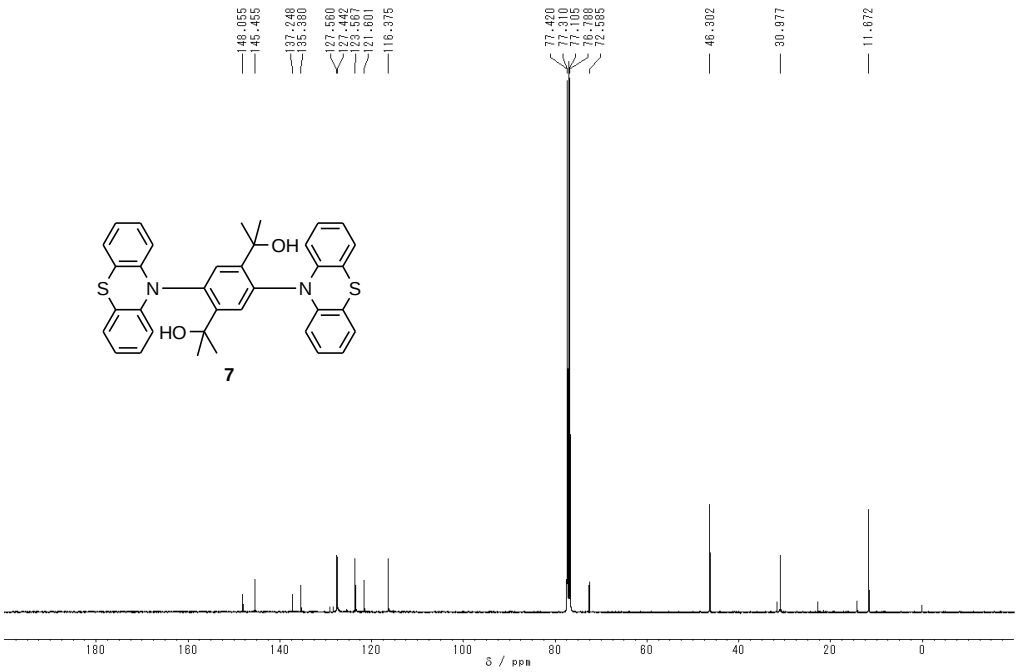

Figure S32. ^{13}C NMR spectrum of **7** in $CDCl_3/Et_3N$ solution (100 MHz).

5. Tables of cartesian coordinates of molecules

Cartesian Coordinates of (*M*,*M*)-**4** Optimized at the ωB97XD/6-311+G(d,p) Level of Theory

Center Number	Atomic Number	Atomic Type	Coordinates (Angstroms) X	Y	Z
1	7	0	-2.423764	1.383803	-0.020965
2	6	0	-3.488904	0.748952	-0.688017
3	6	0	-4.443244	1.516146	-1.354571
4	6	0	-3.566464	-0.647056	-0.686696
5	6	0	-5.482155	0.897639	-2.037439
6	6	0	-4.582755	-1.249983	-1.423041
7	6	0	-5.533821	-0.488184	-2.090700
8	1	0	-6.229987	1.500267	-2.539882
9	1	0	-4.652212	-2.329316	-1.466596
10	1	0	-6.325732	-0.977311	-2.645541
11	6	0	-2.676703	2.547443	0.731219
12	6	0	-2.093983	2.749825	1.982803
13	6	0	-3.566464	3.504170	0.233084
14	6	0	-2.367139	3.902848	2.704933
15	1	0	-1.416464	2.002541	2.378710
16	6	0	-3.866389	4.638620	0.978926
17	6	0	-3.253388	4.850760	2.206854
18	1	0	-1.895857	4.051432	3.669710
19	1	0	-4.573188	5.360606	0.585664
20	1	0	-3.476248	5.746267	2.774536
21	6	0	-1.200410	0.685464	0.057128
22	6	0	0.004740	1.380049	0.039413
23	6	0	-1.219875	-0.711193	0.077854
24	6	0	1.219875	0.711193	0.077854
25	1	0	-0.027216	2.461077	0.001939
26	6	0	-0.004740	-1.380049	0.039413
27	6	0	1.200410	-0.685464	0.057128
28	1	0	0.027216	-2.461077	0.001939
29	6	0	-2.571658	-1.410388	0.185735
30	16	0	-4.259182	3.281626	-1.386275
31	6	0	-2.488999	-2.891602	-0.186561
32	1	0	-2.158276	-3.033350	-1.218600
33	1	0	-1.796560	-3.415683	0.475685
34	1	0	-3.460814	-3.373623	-0.062448
35	6	0	-3.047924	-1.300330	1.655297
36	1	0	-4.031230	-1.765548	1.767423
37	1	0	-2.340080	-1.808946	2.316331
38	1	0	-3.127097	-0.258160	1.972905
39	7	0	2.423764	-1.383803	-0.020965
40	6	0	3.488904	-0.748952	-0.688017
41	6	0	2.676703	-2.547443	0.731219
42	6	0	4.443244	-1.516146	-1.354571
43	6	0	3.566464	0.647056	-0.686696
44	6	0	2.093983	-2.749825	1.982803
45	6	0	3.566464	-3.504170	0.233084
46	6	0	5.482155	-0.897639	-2.037439
47	16	0	4.259182	-3.281626	-1.386275
48	6	0	4.582755	1.249983	-1.423041
49	6	0	2.571658	1.410388	0.185735

50	6	0	2.367139	-3.902848	2.704933
51	1	0	1.416464	-2.002541	2.378710
52	6	0	3.866389	-4.638620	0.978926
53	6	0	5.533821	0.488184	-2.090700
54	1	0	6.229987	-1.500267	-2.539882
55	1	0	4.652212	2.329316	-1.466596
56	6	0	2.488999	2.891602	-0.186561
57	6	0	3.047924	1.300330	1.655297
58	6	0	3.253388	-4.850760	2.206854
59	1	0	1.895857	-4.051432	3.669710
60	1	0	4.573188	-5.360606	0.585664
61	1	0	6.325732	0.977311	-2.645541
62	1	0	2.158276	3.033350	-1.218600
63	1	0	1.796560	3.415683	0.475685
64	1	0	3.460814	3.373623	-0.062448
65	1	0	4.031230	1.765548	1.767423
66	1	0	2.340080	1.808946	2.316331
67	1	0	3.127097	0.258160	1.972905
68	1	0	3.476248	-5.746267	2.774536

Cartesian Coordinates of (*M*,*P*)-**4** (*meso*-**4**) Optimized at the ωB97XD/6-311+G(d,p) Level of Theory

Center Number	Atomic Number	Atomic Type	Coordinates (Angstroms) X	Y	Z
1	7	0	-2.789402	-0.120709	0.028271
2	6	0	-3.512035	-1.280766	0.369578
3	6	0	-4.770519	-1.494936	-0.200665
4	6	0	-5.522556	-2.608175	0.157416
5	6	0	-3.759647	-3.330060	1.620396
6	6	0	-5.011534	-3.538176	1.053319
7	1	0	-6.504855	-2.748160	-0.279601
8	1	0	-3.358693	-4.042124	2.332486
9	1	0	-5.593822	-4.413917	1.313878
10	6	0	-3.472073	1.103154	-0.104203
11	6	0	-2.891495	2.272000	0.398065
12	6	0	-4.708236	1.139650	-0.748148
13	6	0	-3.548620	3.479640	0.177242
14	6	0	-5.375229	2.346860	-0.908937
15	6	0	-4.779015	3.519716	-0.467113
16	1	0	-3.111416	4.405746	0.527728
17	1	0	-6.343596	2.366063	-1.395531
18	1	0	-5.281451	4.468505	-0.614148
19	6	0	-1.379381	-0.076107	0.049808
20	6	0	-0.637723	-1.120009	-0.493404
21	6	0	-0.747324	1.062981	0.553889
22	6	0	0.747325	-1.062978	-0.553906
23	1	0	-1.170536	-1.973208	-0.892502
24	6	0	0.637724	1.120012	0.493386
25	6	0	1.379382	0.076110	-0.049825
26	1	0	1.170537	1.973212	0.892483
27	6	0	-1.612042	2.129158	1.220560
28	16	0	-5.367797	-0.361133	-1.429762
29	6	0	-2.006970	1.616972	2.627499
30	1	0	-2.545297	0.668214	2.570317

31	1	0	-1.110713	1.467121	3.236057
32	1	0	-2.653726	2.345500	3.124335
33	6	0	-0.871668	3.458421	1.377530
34	1	0	-1.503287	4.193097	1.880973
35	1	0	0.014789	3.333629	2.002625
36	1	0	-0.561469	3.867249	0.412349
37	7	0	2.789403	0.120709	-0.028288
38	6	0	3.472069	-1.103156	0.104197
39	6	0	3.512040	1.280766	-0.369578
40	6	0	4.708226	-1.139656	0.748154
41	6	0	2.891491	-2.272001	-0.398073
42	6	0	3.021458	2.200502	-1.297051
43	6	0	4.770521	1.494932	0.200676
44	6	0	5.375212	-2.346869	0.908951
45	16	0	5.367789	0.361123	1.429773
46	6	0	3.548607	-3.479643	-0.177242
47	6	0	1.612044	-2.129154	-1.220577
48	6	0	3.759664	3.330070	-1.620378
49	1	0	2.053180	2.029597	-1.752393
50	6	0	5.522561	2.608172	-0.157391
51	6	0	4.778997	-3.519723	0.467125
52	1	0	6.343574	-2.366075	1.395554
53	1	0	3.111401	-4.405748	-0.527728
54	6	0	0.871668	-3.458414	-1.377559
55	6	0	2.006983	-1.616963	-2.627511
56	6	0	5.011547	3.538180	-1.053291
57	1	0	3.358716	4.042140	-2.332466
58	1	0	6.504857	2.748153	0.279634
59	1	0	5.281427	-4.468515	0.614167
60	1	0	0.561479	-3.867256	-0.412381
61	1	0	-0.014795	-3.333612	-2.002643
62	1	0	1.503282	-4.193083	-1.881019
63	1	0	2.653732	-2.345495	-3.124350
64	1	0	1.110730	-1.467096	-3.236070
65	1	0	2.545322	-0.668211	-2.570320
66	1	0	5.593839	4.413923	-1.313839
67	6	0	-3.021444	-2.200494	1.297055
68	1	0	-2.053162	-2.029585	1.752388

Cartesian Coordinates of (M,R_I) form $_{(TS)}$ of **4** Optimized at the ωB97XD/6-311+G(d,p) Level of Theory

---

Center Number	Atomic Number	Atomic Type	Coordinates (Angstroms) X	Y	Z
1	6	0	-1.383759	0.121478	0.015819
2	6	0	-0.558403	1.251088	0.000792
3	6	0	-0.709679	-1.122153	-0.008988
4	6	0	0.829540	1.210335	0.068943
5	1	0	-0.956004	2.231019	-0.080649
6	6	0	0.674990	-1.165906	0.001834
7	6	0	1.455807	-0.023781	0.071183
8	1	0	1.178995	-2.120276	-0.049041
9	7	0	2.860908	-0.097386	0.042134
10	6	0	3.544466	0.958959	-0.589729
11	6	0	3.580563	-1.032888	0.811151

12	6	0	4.772234	0.716903	-1.204848
13	6	0	2.970938	2.234722	-0.613283
14	6	0	3.094850	-1.499058	2.033140
15	6	0	4.828962	-1.473532	0.361972
16	6	0	5.440767	1.744767	-1.856393
17	16	0	5.418723	-0.936212	-1.223600
18	6	0	3.629891	3.237670	-1.319755
19	6	0	1.698602	2.458649	0.203934
20	6	0	3.827188	-2.416211	2.773684
21	1	0	2.135085	-1.146227	2.391786
22	6	0	5.575713	-2.361742	1.127745
23	6	0	4.853464	2.999635	-1.933247
24	1	0	6.402730	1.553411	-2.317747
25	1	0	3.198780	4.228560	-1.382044
26	6	0	0.964147	3.736951	-0.205250
27	6	0	2.110031	2.587168	1.691682
28	6	0	5.068991	-2.850287	2.325024
29	1	0	3.430028	-2.779491	3.714503
30	1	0	6.550341	-2.678368	0.773747
31	1	0	5.356473	3.799023	-2.464399
32	1	0	0.635866	3.703968	-1.247531
33	1	0	0.093689	3.901758	0.434746
34	1	0	1.607238	4.608789	-0.071518
35	1	0	2.761696	3.454727	1.828482
36	1	0	1.220867	2.709816	2.316703
37	1	0	2.649088	1.700412	2.032902
38	1	0	5.647042	-3.557505	2.907727
39	7	0	-2.832104	0.141826	0.011265
40	6	0	-3.447902	-0.989965	-0.596333
41	6	0	-3.650397	1.289237	0.336440
42	6	0	-4.832892	-1.086614	-0.807848
43	6	0	-2.706644	-2.133100	-0.927402
44	6	0	-3.195252	2.616487	0.404999
45	6	0	-5.031690	1.155773	0.606695
46	6	0	-5.362700	-2.011314	-1.695620
47	16	0	-5.927476	-0.334926	0.343100
48	6	0	-3.235536	-3.062469	-1.823764
49	6	0	-1.491839	-2.412926	-0.068100
50	6	0	-3.968486	3.674245	0.867718
51	1	0	-2.228213	2.907350	0.068405
52	6	0	-5.811065	2.217506	1.056110
53	6	0	-4.537105	-2.959412	-2.283303
54	1	0	-6.431812	-2.012411	-1.874919
55	1	0	-2.627565	-3.899360	-2.140144
56	6	0	-1.993169	-2.757445	1.357018
57	6	0	-0.675088	-3.602190	-0.577945
58	6	0	-5.282923	3.481107	1.241046
59	1	0	-3.518905	4.659637	0.908003
60	1	0	-6.863351	2.033366	1.243724
61	1	0	-4.929946	-3.665734	-3.004200
62	1	0	-2.568407	-1.935540	1.788999
63	1	0	-1.138928	-2.958526	2.010322
64	1	0	-2.632440	-3.644204	1.327642
65	1	0	-1.301793	-4.495176	-0.617624
66	1	0	0.143783	-3.834190	0.105423
67	1	0	-0.259511	-3.420533	-1.572356
68	1	0	-5.896079	4.292721	1.612552

Cartesian Coordinates of (M,S_I) form $_{(TS)}$ of **4** Optimized at the ωB97XD/6-311+G(d,p) Level of Theory

---

Center Number	Atomic Number	Atomic Type	Coordinates (Angstroms) X	Y	Z
1	7	0	-2.829254	0.175122	-0.050366
2	6	0	-3.480360	-1.081909	0.101079
3	6	0	-4.875689	-1.214673	0.191269
4	6	0	-2.761955	-2.285695	0.062409
5	6	0	-5.458539	-2.373600	0.681920
6	6	0	-3.344476	-3.451804	0.560823
7	6	0	-4.670421	-3.482414	0.956914
8	1	0	-6.536375	-2.412368	0.790952
9	1	0	-2.758545	-4.360051	0.605300
10	1	0	-5.106244	-4.382901	1.371805
11	6	0	-3.625300	1.381927	0.001882
12	6	0	-3.164548	2.640138	0.423473
13	6	0	-4.989362	1.379697	-0.369519
14	6	0	-3.910052	3.808289	0.320987
15	1	0	-2.214513	2.777663	0.883468
16	6	0	-5.742223	2.546742	-0.456929
17	6	0	-5.203010	3.784231	-0.160753
18	1	0	-3.456236	4.736777	0.647557
19	1	0	-6.782770	2.461029	-0.750612
20	1	0	-5.793745	4.686890	-0.255379
21	6	0	-1.382973	0.125827	0.010527
22	6	0	-0.554928	1.164875	0.450408
23	6	0	-0.715999	-1.066382	-0.352996
24	6	0	0.832531	1.105518	0.478721
25	1	0	-0.953050	2.068373	0.838129
26	6	0	0.668966	-1.122938	-0.345547
27	6	0	1.456121	-0.053466	0.047156
28	1	0	1.164137	-2.027263	-0.668530
29	6	0	-1.502530	-2.284409	-0.778194
30	16	0	-5.896968	-0.091754	-0.694430
31	6	0	-1.925738	-2.120076	-2.259222
32	1	0	-2.477857	-1.190773	-2.416097
33	1	0	-1.038083	-2.102126	-2.898055
34	1	0	-2.565019	-2.953662	-2.563176
35	6	0	-0.715342	-3.590980	-0.653759
36	1	0	-1.344523	-4.435617	-0.940724
37	1	0	0.136200	-3.601497	-1.335978
38	1	0	-0.348905	-3.755087	0.363063
39	7	0	2.859529	-0.103266	-0.033004
40	6	0	3.530249	1.112637	-0.267132
41	6	0	3.599339	-1.239790	0.350661
42	6	0	4.741852	1.109923	-0.957165
43	6	0	2.960418	2.310933	0.175966
44	6	0	3.148956	-2.099803	1.352598
45	6	0	4.834992	-1.487318	-0.254335
46	6	0	5.397434	2.305398	-1.219840
47	16	0	5.382507	-0.428273	-1.569631
48	6	0	3.605003	3.502459	-0.146432
49	6	0	1.706463	2.222224	1.046143

50	6	0	3.901843	-3.207809	1.714636
51	1	0	2.200084	-1.900445	1.836375
52	6	0	5.603026	-2.576932	0.140629
53	6	0	4.812253	3.503087	-0.834063
54	1	0	6.347226	2.294932	-1.741958
55	1	0	3.176151	4.449249	0.155584
56	6	0	0.968744	3.559882	1.134997
57	6	0	2.147159	1.810814	2.472371
58	6	0	5.130003	-3.450684	1.110940
59	1	0	3.531616	-3.874647	2.484756
60	1	0	6.567738	-2.743193	-0.325342
61	1	0	5.304657	4.441411	-1.060501
62	1	0	0.614502	3.895972	0.156985
63	1	0	0.114107	3.484824	1.812087
64	1	0	1.618763	4.330097	1.554420
65	1	0	2.801574	2.575717	2.899782
66	1	0	1.270688	1.695508	3.116535
67	1	0	2.692360	0.864350	2.463895
68	1	0	5.724081	-4.309226	1.400480

Cartesian Coordinates of (*P*,*P*)-**4** Optimized at the M06-2X/6-31G(d) Level of Theory

Center Number	Atomic Number	Atomic Type	Coordinates (Angstroms) X	Y	Z
1	6	0	5.311235	-1.796638	-1.997745
2	6	0	4.699756	-3.043291	-2.066578
3	6	0	3.484635	-3.263590	-1.423319
4	6	0	2.859737	-2.248241	-0.699743
5	6	0	3.452159	-0.978501	-0.690255
6	6	0	4.674622	-0.755924	-1.328606
7	6	0	1.613997	-2.450406	0.159930
8	6	0	0.745753	-1.202395	0.042139
9	6	0	1.385345	0.043796	0.027350
10	7	0	2.795949	0.088666	-0.041003
11	6	0	-0.644048	-1.225845	0.007006
12	6	0	-1.385283	-0.043843	0.027160
13	6	0	-0.745709	1.202364	0.042063
14	6	0	0.644106	1.225798	0.007152
15	6	0	3.553003	1.004639	0.720572
16	6	0	4.807372	1.416502	0.252563
17	16	0	5.355338	0.884047	-1.350277
18	6	0	3.102118	1.472149	1.959162
19	6	0	3.873672	2.363624	2.695585
20	6	0	5.120365	2.770458	2.227690
21	6	0	5.591223	2.280192	1.013652
22	6	0	2.075224	-2.562172	1.632749
23	6	0	0.853245	-3.723784	-0.208648
24	7	0	-2.795885	-0.088824	-0.041301
25	6	0	-3.452171	0.978417	-0.690358
26	6	0	-2.859800	2.248179	-0.699770
27	6	0	-1.613944	2.450424	0.159726
28	6	0	-4.674718	0.755867	-1.328555
29	6	0	-5.311510	1.796634	-1.997449
30	6	0	-4.700159	3.043351	-2.066123

31	6	0	-3.484950	3.263613	-1.423012
32	6	0	-3.552879	-1.004676	0.720491
33	6	0	-4.807306	-1.416537	0.252599
34	16	0	-5.355371	-0.884128	-1.350227
35	6	0	-3.101937	-1.472134	1.959065
36	6	0	-3.873490	-2.363539	2.695593
37	6	0	-5.120221	-2.770363	2.227824
38	6	0	-5.591140	-2.280147	1.013775
39	6	0	-0.853266	3.723755	-0.209233
40	6	0	-2.075025	2.562440	1.632563
41	1	0	6.269117	-1.617838	-2.476443
42	1	0	5.178370	-3.850500	-2.611327
43	1	0	3.031465	-4.247524	-1.475221
44	1	0	-1.180873	-2.167717	-0.031392
45	1	0	1.180986	2.167633	-0.031163
46	1	0	2.138308	1.137581	2.330453
47	1	0	3.502964	2.727166	3.648735
48	1	0	5.728248	3.457523	2.806824
49	1	0	6.567933	2.573398	0.640406
50	1	0	1.205142	-2.674541	2.289024
51	1	0	2.629690	-1.670413	1.942153
52	1	0	2.728208	-3.432572	1.756641
53	1	0	-0.011340	-3.854480	0.448139
54	1	0	1.489542	-4.602216	-0.070568
55	1	0	0.504742	-3.701678	-1.246119
56	1	0	-6.269449	1.617817	-2.476025
57	1	0	-5.178913	3.850642	-2.610627
58	1	0	-3.031939	4.247628	-1.474748
59	1	0	-2.138090	-1.137616	2.330301
60	1	0	-3.502703	-2.727026	3.648735
61	1	0	-5.728093	-3.457373	2.807032
62	1	0	-6.567888	-2.573337	0.640616
63	1	0	-1.489787	4.602156	-0.071991
64	1	0	-0.504232	3.701064	-1.246508
65	1	0	0.010939	3.855104	0.447914
66	1	0	-2.728223	3.432692	1.756332
67	1	0	-1.204900	2.675164	2.288718
68	1	0	-2.629216	1.670588	1.942208

Cartesian Coordinates of *meso*-**4**$^{\bullet+}$ Optimized at the UM06-2X/6-31G(d) Level of Theory

Center Number	Atomic Number	Atomic Type	Coordinates (Angstroms) X	Y	Z
1	6	0	0.652349	-1.185100	-0.339032
2	6	0	-0.714179	-1.139257	-0.476265
3	6	0	-1.382302	0.063101	-0.117565
4	6	0	-0.652350	1.185099	0.339033
5	6	0	0.714179	1.139257	0.476266
6	6	0	1.382301	-0.063102	0.117567
7	7	0	2.757723	-0.089429	0.159975
8	7	0	-2.757723	0.089429	-0.159972
9	6	0	3.464483	1.131343	-0.010716
10	6	0	4.703669	1.128047	-0.658002
11	16	0	5.396397	-0.352552	-1.324535

12	6	0	4.712571	-1.516508	-0.191926
13	6	0	3.473911	-1.288215	0.418897
14	6	0	-3.464485	-1.131344	0.010715
15	6	0	-4.703671	-1.128048	0.657999
16	16	0	-5.396397	0.352551	1.324536
17	6	0	-4.712571	1.516508	0.191928
18	6	0	-3.473910	1.288215	-0.418894
19	6	0	5.405557	-2.697821	0.077811
20	6	0	4.874049	-3.639071	0.949071
21	6	0	3.658584	-3.392231	1.589294
22	6	0	2.967974	-2.217132	1.337374
23	6	0	2.862959	2.327142	0.405891
24	6	0	3.533789	3.520512	0.160129
25	6	0	4.778214	3.525323	-0.469238
26	6	0	5.367216	2.336141	-0.872024
27	6	0	-2.862961	-2.327142	-0.405895
28	6	0	-3.533792	-3.520512	-0.160136
29	6	0	-4.778218	-3.525323	0.469229
30	6	0	-5.367220	-2.336142	0.872017
31	6	0	-5.405556	2.697822	-0.077808
32	6	0	-4.874045	3.639073	-0.949066
33	6	0	-3.658579	3.392234	-1.589286
34	6	0	-2.967970	2.217133	-1.337367
35	6	0	1.535582	2.231628	1.148350
36	6	0	-1.535583	-2.231628	-1.148351
37	6	0	0.793821	3.567457	1.191158
38	6	0	1.826969	1.780117	2.601609
39	6	0	-1.826966	-1.780117	-2.601612
40	6	0	-0.793822	-3.567458	-1.191158
41	1	0	1.204358	-2.065912	-0.644929
42	1	0	-1.204358	2.065911	0.644929
43	1	0	6.369409	-2.864327	-0.392973
44	1	0	5.421220	-4.553567	1.150931
45	1	0	3.259749	-4.106424	2.301246
46	1	0	2.036823	-2.002319	1.852782
47	1	0	3.092193	4.462790	0.462610
48	1	0	5.290263	4.465563	-0.643272
49	1	0	6.336157	2.333620	-1.361113
50	1	0	-3.092196	-4.462790	-0.462619
51	1	0	-5.290268	-4.465563	0.643260
52	1	0	-6.336161	-2.333621	1.361105
53	1	0	-6.369408	2.864328	0.392974
54	1	0	-5.421215	4.553569	-1.150925
55	1	0	-3.259742	4.106428	-2.301236
56	1	0	-2.036818	2.002321	-1.852773
57	1	0	1.397706	4.321224	1.701553
58	1	0	0.552953	3.931588	0.187295
59	1	0	-0.131615	3.474854	1.765669
60	1	0	2.439750	2.534096	3.104462
61	1	0	0.888529	1.661972	3.152360
62	1	0	2.368466	0.829148	2.628576
63	1	0	-2.439746	-2.534096	-3.104465
64	1	0	-2.368462	-0.829148	-2.628580
65	1	0	-0.888524	-1.661974	-3.152360
66	1	0	-1.397707	-4.321224	-1.701554
67	1	0	0.131615	-3.474855	-1.765667
68	1	0	-0.552956	-3.931588	-0.187295

Cartesian Coordinates of **TPPD** Optimized at the M06-2X/6-31G(d) Level of Theory

---

Center Number	Atomic Number	Atomic Type	Coordinates (Angstroms) X	Y	Z
1	7	0	-2.823702	0.000121	0.001277
2	6	0	-3.529843	1.226199	-0.026775
3	6	0	-3.529015	-1.226650	0.028029
4	6	0	0.694209	-0.887441	0.811727
5	6	0	-3.065738	2.329021	0.699118
6	6	0	-1.407228	0.000237	0.000180
7	6	0	-4.700425	1.352384	-0.784160
8	6	0	-0.693546	-0.886849	0.812847
9	6	0	-3.065530	-2.327528	-0.701025
10	6	0	-5.394804	2.556154	-0.802950
11	6	0	-4.698174	-1.355056	0.787191
12	6	0	-5.391576	-2.559424	0.805323
13	6	0	-3.756873	-3.533193	-0.661601
14	6	0	-4.925150	-3.657328	0.086045
15	6	0	-4.928011	3.655902	-0.086634
16	6	0	-3.758060	3.534162	0.658764
17	7	0	2.823793	-0.000307	-0.002516
18	6	0	3.530165	-1.226178	0.024074
19	6	0	3.528718	1.226734	-0.026362
20	6	0	-0.694151	0.886793	-0.813675
21	6	0	3.065725	-2.328563	-0.702304
22	6	0	1.407267	-0.000801	-0.001966
23	6	0	4.701241	-1.352725	0.780590
24	6	0	0.693613	0.886173	-0.814781
25	6	0	3.063505	2.326376	0.703448
26	6	0	5.395708	-2.556458	0.798144
27	6	0	4.699486	1.356498	-0.782846
28	6	0	5.392647	2.561053	-0.797717
29	6	0	3.754630	3.532257	0.667258
30	6	0	4.924424	3.657782	-0.077789
31	6	0	4.928557	-3.655810	0.081455
32	6	0	3.758117	-3.533689	-0.663120
33	1	0	1.237894	-1.573173	1.454566
34	1	0	-2.160289	2.233085	1.290494
35	1	0	-5.058448	0.499832	-1.352994
36	1	0	-1.236858	-1.572307	1.456320
37	1	0	-2.161615	-2.229534	-1.294410
38	1	0	-6.302101	2.635800	-1.394369
39	1	0	-5.055431	-0.503867	1.358553
40	1	0	-6.297226	-2.641168	1.398970
41	1	0	-3.384004	-4.377948	-1.233252
42	1	0	-5.465689	-4.597917	0.107956
43	1	0	-5.469520	4.595930	-0.109241
44	1	0	-3.384618	4.380282	1.228032
45	1	0	-1.237820	1.572780	-1.456251
46	1	0	2.159882	-2.232281	-1.293028
47	1	0	5.059545	-0.500523	1.349778
48	1	0	1.236980	1.571880	-1.457954
49	1	0	2.158401	2.227212	1.294830

50	1	0	6.303407	-2.636401	1.388912
51	1	0	5.058259	0.506167	-1.354540
52	1	0	6.299582	2.643889	-1.389253
53	1	0	3.380362	4.376070	1.239384
54	1	0	5.464781	4.598531	-0.097170
55	1	0	5.470199	-4.595780	0.103134
56	1	0	3.384362	-4.379448	-1.232724

Cartesian Coordinates of **TPPD**$^{\bullet+}$ Optimized at the UM06-2X/6-31G(d) Level of Theory

Center Number	Atomic Number	Atomic Type	Coordinates (Angstroms) X	Y	Z
1	7	0	-2.782890	0.000049	0.000080
2	6	0	-3.529154	1.220376	-0.051507
3	6	0	-3.529128	-1.220335	0.051554
4	6	0	0.683995	-1.115816	0.494323
5	6	0	-3.228788	2.258253	0.832970
6	6	0	-1.416817	0.000030	0.000019
7	6	0	-4.578516	1.339454	-0.964027
8	6	0	-0.683991	-1.115784	0.494321
9	6	0	-3.229261	-2.257835	-0.833499
10	6	0	-5.318570	2.515077	-0.999179
11	6	0	-4.577973	-1.339731	0.964633
12	6	0	-5.318044	-2.515338	0.999724
13	6	0	-3.976548	-3.429650	-0.787852
14	6	0	-5.019000	-3.560774	0.127364
15	6	0	-5.019006	3.560861	-0.127432
16	6	0	-3.976045	3.430063	0.787266
17	7	0	2.782917	-0.000052	-0.000060
18	6	0	3.529174	-1.220376	0.051642
19	6	0	3.529139	1.220333	-0.051679
20	6	0	-0.683959	1.115817	-0.494275
21	6	0	3.228766	-2.258355	-0.832700
22	6	0	1.416847	-0.000035	0.000014
23	6	0	4.578550	-1.339366	0.964158
24	6	0	0.684028	1.115778	-0.494286
25	6	0	3.229190	2.257976	0.833178
26	6	0	5.318587	-2.514996	0.999435
27	6	0	4.578027	1.339603	-0.964725
28	6	0	5.318074	2.515220	-0.999970
29	6	0	3.976457	3.429800	0.787378
30	6	0	5.018958	3.560794	-0.127799
31	6	0	5.018989	-3.560877	0.127813
32	6	0	3.976009	-3.430169	-0.786875
33	1	0	1.219896	-1.955555	0.921939
34	1	0	-2.429194	2.134324	1.557453
35	1	0	-4.802347	0.517263	-1.636809
36	1	0	-1.219938	-1.955485	0.921959
37	1	0	-2.430044	-2.133650	-1.558354
38	1	0	-6.129953	2.615208	-1.712231
39	1	0	-4.801337	-0.517793	1.637887
40	1	0	-6.128989	-2.615782	1.713225
41	1	0	-3.752926	-4.235139	-1.479431
42	1	0	-5.603176	-4.474438	0.155880

43	1	0	-5.603170	4.474531	-0.155999
44	1	0	-3.751977	4.235833	1.478371
45	1	0	-1.219854	1.955559	-0.921890
46	1	0	2.429153	-2.134500	-1.557174
47	1	0	4.802403	-0.517102	1.636844
48	1	0	1.219981	1.955483	-0.921910
49	1	0	2.429929	2.133897	1.558003
50	1	0	6.129981	-2.615057	1.712484
51	1	0	4.801441	0.517562	-1.637837
52	1	0	6.129053	2.615565	-1.713446
53	1	0	3.752777	4.235400	1.478809
54	1	0	5.603116	4.474466	-0.156435
55	1	0	5.603138	-4.474552	0.156479
56	1	0	3.751912	-4.236017	-1.477880

---

6. References

1. Frisch, M. J.; Trucks, G. W.; Schlegel, H. B.; Scuseria, G. E.; Robb, M. A.; Cheeseman, J. R.; Scalmani, G.; Barone, V.; Mennucci, B.; Petersson, G. A.; Nakatsuji, H.; Caricato, M.; Li, X.; Hratchian, H. P.; Izmaylov, A. F.; Bloino, J.; Zheng, G.; Sonnenberg, J. L.; Hada, M.; Ehara, M.; Toyota, K.; Fukuda, R.; Hasegawa, J.; Ishida, M.; Nakajima, T.; Honda, Y.; Kitao, O.; Nakai, H.; Vreven, T.; Montgomery, J. A., Jr.; Peralta, J. E.; Ogliaro, F.; Bearpark, M.; Heyd, J. J.; Brothers, E.; Kudin, K. N.; Staroverov, V. N.; Kobayashi, R.; Normand, J.; Raghavachari, K.; Rendell, A.; Burant, J. C.; Iyengar, S. S.; Tomasi, J.; Cossi, M.; Rega, N.; Millam, J. M.; Klene, M.; Knox, J. E.; Cross, J. B.; Bakken, V.; Adamo, C.; Jaramillo, J.; Gomperts, R.; Stratmann, R. E.; Yazyev, O.; Austin, A. J.; Cammi, R.; Pomelli, C.; Ochterski, J. W.; Martin, R. L.; Morokuma, K.; Zakrzewski, V. G.; Voth, G. A.; Salvador, P.; Dannenberg, J. J.; Dapprich, S.; Daniels, A. D.; Farkas, Ö.; Foresman, J. B.; Ortiz, J. V.; Cioslowski, J.; Fox, D. J. *Gaussian 09*; Revision D.01; Gaussian Inc.: Wallingford CT, 2009.
2. CrysAlisPro; Rigaku OD, The Woodlands, TX, 2015.
3. Dolomanov, O. V.; Bourhis, L. J.; Gildea, R. J; Howard, J. A. K.; Puschmann, H. *J. Appl. Cryst.* **2009**, *42*, 339.
4. Sheldrick, G. M. *Acta Crystallogr., Sect. A* **2015**, *71*, 3.
5. Sheldrick, G. M. *Acta Crystallogr., Sect. C* **2015**, *71*, 3.
6. Kato, S.-i.; Matsuoka, T.; Suzuki, S.; Asano, M. S.; Yoshihara, T.; Tobita, S.; Matsumoto, T.; Kitamura, C. *Org. Lett.* **2020**, *22*, 734.
7. Kataoka, S.; Suzuki, S.; Shiota, Y.; Yoshizawa, K.; Matsumoto, T.; Asano, M. S.; Yoshihara, T.; Kitamura, C.; Kato, S.-i. *J. Org. Chem.* **2021**, *86*, 12559.
8. Sun, D.; Rosokha, S. V.; Kochi, J. K. *J. Am. Chem. Soc.* **2004**, *126*, 1388.
9. Szeghalmi, A. V.; Erdmann, M.; Engel, V.; Schmitt, M.; Amthor, S.; Kriegisch, V.; Nöll, G.; Stahl, R.; Lambert, C.; Leusser, D.; Stalke, D.; Zabel, M.; Popp, J. *J. Am. Chem. Soc.* **2004**, *126*, 7834.
10. K. Yamaguchi, T. Kawakami, Y. Takano, Y. Kitagawa, Y. Yamashita, H. Fujita, *Int. J. Quantum Chem*., **2002**, *90*, 370.

7. Author contributions

S.-i. Kato and C. Kitamura conceived and designed the projects; K. Harada synthesized the compounds and contributed on most of the experimental work; C. Hasegawa and M. Hasegawa performed the optical resolution and the UV–vis and CD spectroscopic measurements; K. Harada and S. Higashibayashi performed the kinetic study; K. Harada and H. Sugishita performed the electrochemical measurements; S.-i. Kato and S. Higashibayashi performed the theoretical calculations; T. Matsumoto performed the single-crystal X-ray diffraction analyses; S. Suzuki performed the EPR spectroscopic measurements; S.-i. Kato, S. Higashibayashi, M. Hasegawa, and S. Suzuki wrote the manuscript; S.-i. Kato played a critical role in the discussion of the experimental design, project direction, experiments and results, and preparation of the manuscript; All authors discussed the results and commented on the manuscript.